Biochimica et Biophysica Acta 1793 (2009) 1901–1916

Contents lists available at ScienceDirect

Biochimica et Biophysica Acta

journal homepage: www.elsevier.com/locate/bbamcr

TI-VAMP/VAMP7 and VAMP3/cellubrevin: two v-SNARE proteins involved in specific steps of the autophagy/multivesicular body pathways

Claudio Marcelo Fader [1], Diego Germán Sánchez [1], María Belén Mestre, María Isabel Colombo *

Laboratorio de Biología Celular y Molecular, Instituto de Histología y Embriología (IHEM)-CONICET, Facultad de Ciencias Médicas, Universidad Nacional de Cuyo, Casilla de Correo 56, Centro Universitario, Parque General San Martín, (5500) Mendoza, Argentina

ARTICLE INFO

Article history:
Received 21 August 2009
Accepted 14 September 2009
Available online 23 September 2009

Keywords:
SNAREs
VAMP7
VAMP3
Multivesicular bodies
Autophagy
Autophagosome
Exosomes
LC3
Rab11
K562

ABSTRACT

During reticulocyte maturation, some membrane proteins and organelles that are not required in the mature red cell are lost. Several of these proteins are released into the extracellular medium associated with the internal vesicles present in multivesicular bodies (MVBs). Likewise, organelles such as mitochondria and endoplasmic reticulum are wrapped into double membrane vacuoles (i.e., autophagosomes) and degraded via autophagy. Morphological, molecular, and biochemical studies have shown that autophagosomes fuse with MVBs forming the so-called amphisomes, a prelysosomal hybrid organelle. SNAREs are key molecules of the vesicle fusion machinery. TI-VAMP/VAMP7 and VAMP3/cellubrevin are two v-SNARE proteins involved in the endocytic and exocytic pathways. We have previously shown that in the human leukemic K562 cells, Rab11 decorates MVBs and it is necessary for fusion between autophagosomes with MVBs. In the present report, we present evidence indicating that VAMP3 is required for the fusion between MVBs with autophagosomes to generate the amphisome, allowing the maturation of the autophagosome, but it does not seem to be involved in the next step, i. e., fusion with the lysosome. On the other hand, we demonstrate that VAMP7 is necessary for this latter event, allowing the completion of the autophagic pathway. Furthermore, VAMP7 and ATPase NSF, a protein required for SNAREs disassembly, participate in the fusion between MVBs with the plasma membrane to release the internal vesicles (i.e., exosomes) into the extracellular medium.

1. Introduction

K562 is a cell line derived from a patient who had chronic myeloid leukemia, and these cells are an excellent tool to study multivesicular bodies (MVBs) formation and exosome secretion [1,2]. During erythroid maturation, some plasma membrane proteins are selectively sorted by inward budding and the subsequent pinching off of the endosomal membrane into the luminal space, leading to the formation of multivesicular bodies (MVBs), which accumulate internally small membrane vesicles (60–80 nm). These intraluminal vesicles once released into the extracellular medium by fusion of MVBs with the plasma membrane are known as exosomes [3–8].

The main physiological pathway for degradation of intracellular macromolecules in eukaryotic cells is autophagy [9,10]. This intracellular process plays a key role in the turnover of long-lived proteins, RNA, cytoplasmic macromolecules, and also organelles [11–13]. This degradation process of superfluous organelles has been also associated with red blood cell maturation [14–16]. During autophagy, parts of the cytoplasm and organelles are encapsulated in double membrane vacuoles called autophagosomes, which subsequently fuse with lysosomes to degrade the incorporated material (for a review, see Shintani and Klionsky [17]). Several reports have shown the convergence between the endocytic and autophagic pathways. It has been visualized by electron microscopy that MVBs deliver their endocytosed markers to the early autophagosomes where the two pathways meet [18]. Although the molecular machinery that participates in trafficking and convergence between both autophagy and MVBs pathway has not been fully uncovered, some of the proteins involved in this event have been recently elucidated [19]. Moreover, in a recent publication, it has demonstrated that isolated autophagic vacuoles can fuse, in vitro, with both early and late endosomes [20].

Genetic studies in yeast have shown that the combined action of a group of class E (Vps) proteins termed ESCRT I, II, and III (endosomal sorting complexes required for transport) is necessary for MVB biogenesis. Many of these Vps proteins are recruited from the cytoplasm to the endosomal membrane in a sequential form [21–24]. Another important factor that regulates and coordinates the biogenesis of MVB is Hrs (hepatocyte growth factor-regulated tyrosine kinase substrate), which is able to bind ubiquitylated proteins [25–29]. Interestingly, recent publications have shown that autophagy degradation is abrogated in cells depleted for ESCRT subunits or in cells overexpressing a mutant of CHMP2B (charged multivesicular body protein 2B/chromatin-modifying protein 2B), which caused an accumulation of ubiquitin–protein aggregates [30,31], establishing a connection

* Corresponding author. Tel.: +54 261 4494143; fax: +54 261 4494117.
E-mail address: mcolombo@fcm.uncu.edu.ar (M.I. Colombo).
[1] Both authors contributed equally to this work.

0167-4889/$ – see front matter © 2009 Elsevier B.V. All rights reserved.
doi:10.1016/j.bbamcr.2009.09.011

between autophagy and MVBs at the molecular level (for a review, see Fader and Colombo and Rusten and Simonsen [32,33]).

Protein trafficking in the endocytic and secretory pathway requires a series of events including cargo selection and vesicle budding at the donor organelle, followed by transport, docking, and fusion of vesicles with its proper target organelle. Yeast and mammalian cells appear to share highly conserved machinery that participates in protein sorting and membrane fusion. The main model for targeting of the cargo to a suitable destination is focused in the role of the SNARE complex, which postulates that during neuronal exocytic events, an interaction between VAMP/synaptobrevin (v-SNARE) and syntaxin (t-SNARE) molecules provides the specificity required [34]. This complex also needs a stable interaction with an additional t-SNARE (SNAP-25), which forms a complex with syntaxin. SNARE proteins contain a specific region (SNARE motifs) that contribute to the formation of a highly stable four-helix bundle, termed the SNARE complex. Each SNARE motif contributes to the formation of this four alfa-helix bundle, which are all aligned in parallel [34–36]. The folding of this bundle is thought to drive membrane to the fusion event. Initially, the SNARE complex has a *trans*-configuration, where the SNARE proteins involved in the formation of the complex are localized in different membranes. Subsequently, the complete SNARE complex temporally coincides with membrane fusion, resulting in the formation of a *cis*-complex because all of the SNARE proteins are localized to the same membrane. Finally, the ternary *cis*-complex is disassembled by the chaperone ATPase NSF (*N*-ethyl-maleimide-sensitive factor) in conjunction with SNAPs (soluble *N*-ethyl-maleimide attachment proteins) proteins [34,37].

Clostridial neurotoxins (NTs) carry a proteolytic activity that selectively cleaves defined SNARES. Hence, these toxins have been extensively used to demonstrate the involvement of NTs-sensitive SNAREs in vesicular transport (see review [38]). However, cumulative evidence indicates the participation of SNAREs insensitive to neurotoxins in specific transport events. It is believed that tetanus neurotoxin-insensitive VAMP proteins are involved in the constitutive exocytosis of neurons, since the neurotoxin completely inhibited the regulated neurotransmitter release but not neurite outgrowth [39,40]. Indeed, a VAMP tetanus toxin-insensitive, designated as TI-VAMP [41] or VAMP7 [42], was identified. TI-VAMP/VAMP7 has a long N-terminal extension (90 amino acids) compared with other VAMP family proteins. Interestingly, this N-terminal extension produces an inhibitory effect on the SNARE complex formation, and the expression of this domain inhibits neurite outgrowth in neurons and PC12 cells in culture [43]. VAMP7 is also believed to be involved in apical transport of constitutive vesicles in polarized epithelial cells, such as MDCK cells and CaCo-2 cells [41]. Moreover, it has been shown that TI-VAMP/VAMP7 is localized in late endosomes and is thought to function as a v-SNARE for endosomal vesicle trafficking to lysosomes [42,44]. On the other hand, it has been recently demonstrated that VAMP7 is involved in constitutive exocytosis in HSY cells [45]. Nevertheless, the physiological roles and distribution of TI-VAMP/VAMP7 in intracellular vesicle trafficking are still not clear.

VAMP3/cellubrevin has been postulated to be a v-SNARE for early and recycling endosomes and probably for constitutive exocytosis, but mice with a null mutation of this gene were normal in most endocytic and exocytic pathways including constitutive exocytosis [46,47]. Thus, the actual role of VAMP3 in both pathways is not completely understood.

In the present report, we provide evidence suggesting that VAMP7 is a v-SNARE that participates in the fusion between MVBs with plasma membrane to release exosomes into the extracellular medium. Furthermore, we demonstrate that VAMP7 is required for the last step of the autophagic process (i.e., fusion with the lysosomes). On the other hand, our results indicate that VAMP3 is necessary for the fusion of MVBs with autophagosomes to generate the hybrid organelle termed amphisome, allowing the maturation of the autophagosome.

2. Materials and methods

2.1. Materials

RPMI cell culture medium and fetal calf serum were obtained from Invitrogen Argentina S.A. (Buenos Aires, Argentina). *N*-(lissamine rhodamine B sulfonyl)-phosphatidylethanolamine (N-Rh-PE) was obtained from Avanti Polar Lipids, Inc. (Birmingham, AL). Acetylthiocholine and 5,5′-dithio-*bis*(2-nitrobenzoic acid) were obtained from Sigma (Buenos Aires, Argentina). *N*-ethylmaleimide was obtained from Sigma (Buenos Aires, Argentina).

2.2. Plasmids

The pEGFP-LC3wt was kindly provided by Dr. Noboru Mizushima (Tokyo Medical and Dental University, Tokyo, Japan). The insert encoding the LC3 protein was subcloned into the red fluorescent protein vector (pRFP, kindly provided by Dr. Philip Stahl, Washington University, St. Louis, MO). Briefly, the insert from pEGFP-LC3wt was cut with the *Bgl*II and *Eco*RI restriction enzymes and subcloned in the corresponding restriction sites of pRFP vector. The pEGFPRab11 plasmids were used as previously described [48]. The insert corresponding to Rab11wt was also subcloned in the pRFP vector. pEGFPC3 encoding GFP-VAMP3, GFP-TI-VAMP, or GFP-Longin domain was kindly provided by Dr. Thierry Galli (Institut Jacques Monod, Paris, France) and have been described previously [43]. pCMV5-TeNT was kindly provided by Dr. Heiner Niemann (Hannover Medical School, Hannover, Germany) and Dr. Jochen Lang (Institut Européen de Chimie et Biologie, Bordeaux, France).

2.3. Cell culture and transfection

K562, an erythroleukemia cell line of human origin, was grown in RPMI supplemented with 10% FCS, streptomycin (50 μg/ml) and penicillin (50 U/ml). For some experiments, cells were incubated in starvation media EBSS (Earle's balanced salt solution). Stably transfected K562 cells overexpressing pEGFP (control) or pEGFP-Rab11wt-generated previously [48] were used. For some experiments, K562 cells were transfected with pRFP-LC3, the stable transfectants were selected with geneticin (0.5 mg/ml) and subsequently cloned. K562 cells were also transiently transfected with pEGFP-Rab11wt, pEGFP-VAMP3, pEGFP-VAMP7, pEGFP-NT-VAMP7, or cotransfected with pRFP-Rab11wt/pEGFP-VAMP3, pRFP-Rab11wt/pEGFP-VAMP7, pRFP-Rab11wt/ pEGFP-NT-VAMP7, and pRFP-LC3/ pEGFP-VAMP3, using DMRIE-C (Invitrogen Argentina S.A.), according to the manufacturer's instructions or by electroporation, following standard procedures.

2.4. Labeling with N-Rh-PE

The fluorescent phospholipid analog N-Rh-PE was inserted into the plasma membrane as previously described. Briefly, an appropriate amount of the lipid, stored in chloroform/methanol (2:1), was dried under nitrogen and subsequently solubilized in absolute ethanol. This ethanolic solution was injected with a Hamilton syringe into serum-free RPMI (<1% v/v) while vigorously vortexing. The mixture was then added to the cells, and they were incubated for 60 min at 4 °C. After this incubation period, the medium was removed, and the cells were extensively washed with cold PBS to get rid of excess unbound lipids. Labeled cells were cultured in complete RPMI medium under several conditions allowing the internalized lipid to reach the MVBs. After this incubation, cells were washed in PBS and immediately mounted on coverslips and analyzed by confocal microscopy.

To label endocytic compartments at different times after internalization, cells incubated for 60 min at 4 °C with N-Rh-PE as indicated above were washed, centrifuged for 2 min at 400×*g* and incubated in suspension at 37 °C, 5% CO_2. At different time points, the cells were

placed on ice, washed once with cold PBS, and immediately mounted on coverslips and analyzed by confocal microscopy.

2.5. Test of lysosomal function by degradation of a chromogenic BSA

The ability of K562 cells to endocytose and degrade the self-quenched red Bodipy dye conjugated to BSA (DQ-BSA, Molecular Probes, Eugene, OR) was used to measure lysosome function. Red DQ-BSA requires enzymatic cleavage in an acidic intracellular compartment to generate a highly fluorescent product, which can be monitored by confocal microscopy. K562 cells were incubated for 12 h at 37 °C with DQ-BSA (10 μg/ml in RPMI containing 10% fetal bovine serum) to ensure that the reagent reaches the lysosomal compartment. Cells were then washed twice with PBS and incubated in starvation media under different experimental conditions.

2.6. Immunoelectron microscopy

K562 cells overexpressing pGFP-LC3 were incubated for 3 h at 37 °C in full nutrient or in amino acid and serum-free media in presence or absence of pCMV5-TeNT plasmid. Cells were fixed in 4% paraformaldehyde in 0,2 M phosphate buffer, pH 7.4 (PB) for 2 h at 4 °C. After washing with PB and PB containing 50 mM glycine, cells were embedded in 10% gelatine. Small blocks were infiltrated with 2.3 M sucrose at 4 °C for 2 h and then frozen in liquid nitrogen. Ultrathin cryosections were prepared with a Leica ultracut R, retrieved with a mixture of 2% methylcellulose and 2.3 M sucrose (vol/vol). Seventy-nanometer sections were sequentially labeled with mouse anti-LBPA antibody, followed by a rabbit anti-mouse antibody (Molecular Probes). The rabbit antibodies were detected with protein A coupled to 5-nm gold particles (kindly provided by Dr. Gareth Griffith). Subsequently, the samples were incubated with a rabbit anti-GFP (Abcam, Cambridge), which was detected with protein A coupled to 15-nm gold particles. To fix the first immunocomplex and to avoid the possible cross-reaction, 1% glutaraldehyde was added at the end of the first labeling procedure. The sections were contrasted and embedded in a mixture of methylcellulose and uranyl acetate and viewed under a Zeiss 900 electron microscope.

2.7. Indirect immunofluorescence for endogenous LC3 and Rab11 proteins

Cells were attached to polylysine-coated coverslips and fixed with 1 ml of 3% paraformaldehyde solution in PBS for 30 min at room temperature. Samples were washed several times with PBS and blocked by incubating with 50 mM NH_4Cl for 15 min in PBS. Cells were permeabilized with 0.05% saponin in PBS containing 0.2% BSA and were incubated with an affinity-purified mouse antibody against LC3 (dilution 1:50), a rabbit antibody against Rab11 (dilution 1:50), in PBS containing 1% BSA. Bound antibodies were subsequently detected by incubation with Cy3 goat–anti-mouse secondary antibody (dilution 1:600, Jackson ImmunoResearch, West Grove, PA) and Alexa Fluor 488-labeled goat–anti-rabbit secondary antibody (dilution 1:500, Molecular Probes, Eugene, OR). Samples were mounted with 50% glycerol in PBS and analyzed by confocal microscopy.

2.8. Exosome isolation

Exosomes were collected from 10 ml of K562 media (15–20×106 cells) cultured for approximately 15 h. The culture medium was collected on ice, centrifuged at 800×*g* for 10 min to sediment the cells, and then centrifuged at 12,000×*g* for 30 min to remove the cellular debris. Exosomes were separated from the supernatant by centrifugation at 100,000×*g* for 2 h. The exosome pellet was washed once in a large volume of PBS and resuspended in 100 μl of PBS (exosome fraction).

2.9. Quantitation of released exosomes

2.9.1. Acetylcholinesterase assay

The amount of released exosomes was quantitated by measuring the activity of acetylcholinesterase, an enzyme that is specifically directed to these vesicles. Acetylcholinesterase activity was assayed following a previously described procedure. Briefly, 25 μl of the exosome fraction was suspended in 100 μl of phosphate buffer and incubated with 1.25 mM acetylthiocholine and 0.1 mM 5,5′-dithiobis (2-nitrobenzoic acid) in a final volume of 1 ml. The incubation was carried out in cuvettes at 37 °C, and the change in absorbance at 412 nm was followed continuously. The data represent the enzymatic activity at 20 min of incubation.

2.10. Fluorescent N-Rh-PE measurement

The fluorescent phospholipid analog *N*-(lissamine rhodamine B sulfonyl) phosphatidyl ethanolamine (N-Rh-PE) was inserted into the plasma membrane as previously described. Briefly, an appropriate amount of the lipid, stored in chloroform/methanol (2:1), was dried under nitrogen and subsequently solubilized in absolute ethanol. This ethanolic solution was injected with a Hamilton syringe into serum-free RPMI (<1% v/v) while vigorously vortexing. The mixture was then added to the cells, and they were incubated for 60 min at 4 °C. After this incubation period, the medium was removed, and the cells were extensively washed with cold PBS to remove excess unbound lipids. Labeled cells were cultured in complete RPMI medium to collect exosomes. Fifty milliliter of the exosomal fraction was solubilized with 1.5 ml PBS containing 0.1% Triton X-100 to measure N-Rh-PE using a SLM Aminco Bowman Series 2 luminescence spectrometer at 560 nm and 590 nm excitation and emission wavelengths, respectively.

2.11. Statistical analysis

Results are represented as the mean ± SEM from at least two independent experiments. The comparisons were performed using ANOVA in conjunction with Tukey and Dunnett tests. Significant differences were $^{*}P<0.01$; $^{**}P<0.005$.

3. Results

3.1. GFP-VAMP7 but not GFP-VAMP3 decorates large MVBs in K562 cells

Like reticulocytes, K562 cells generate multivesicular bodies (MVBs) and release small vesicles termed exosomes into the extracellular medium after fusion of MVBs with the plasma membrane [6]. To investigate the possible role of SNARE proteins on the MVBs pathway, we analyzed this process in transiently transfected K562 cells overexpressing GFP-VAMP3 or GFP-VAMP7, two v-SNAREs involved in the endocytic pathway [35,49–52]. To specifically label the MVBs, cells were incubated for 1 h with the fluorescent lipid analog N-Rh-PE, which is efficiently incorporated into the internal vesicles (i.e., exosomes) [53]. As shown in Fig. 1A, panels a–c, GFP-VAMP3 presented a punctate vesicular pattern but no colocalization with N-Rh-PE-labeled MVBs was observed. In contrast, MVBs were clearly decorated by GFP-VAMP7 (panels d–f). Interestingly, overexpression of GFP-VAMP7 generated an enlargement of the MVBs decorated with this protein (panels d–f).

As mentioned above, our results indicate that VAMP3 does not colocalize with MVBs labeled with the lipid N-Rh-PE internalized for a 1-h period. However, since VAMP3 is one of the v-SNARE required for early and recycling endosomes [47], we were interested in investigating the relationship between VAMP3 and the early steps of the endocytic pathway in K562 cells. For this purpose, we analyzed the distribution of N-Rh-PE in cells overexpressing GFP-VAMP3 at different times after internalization. As shown in Fig. 1B, a subset of

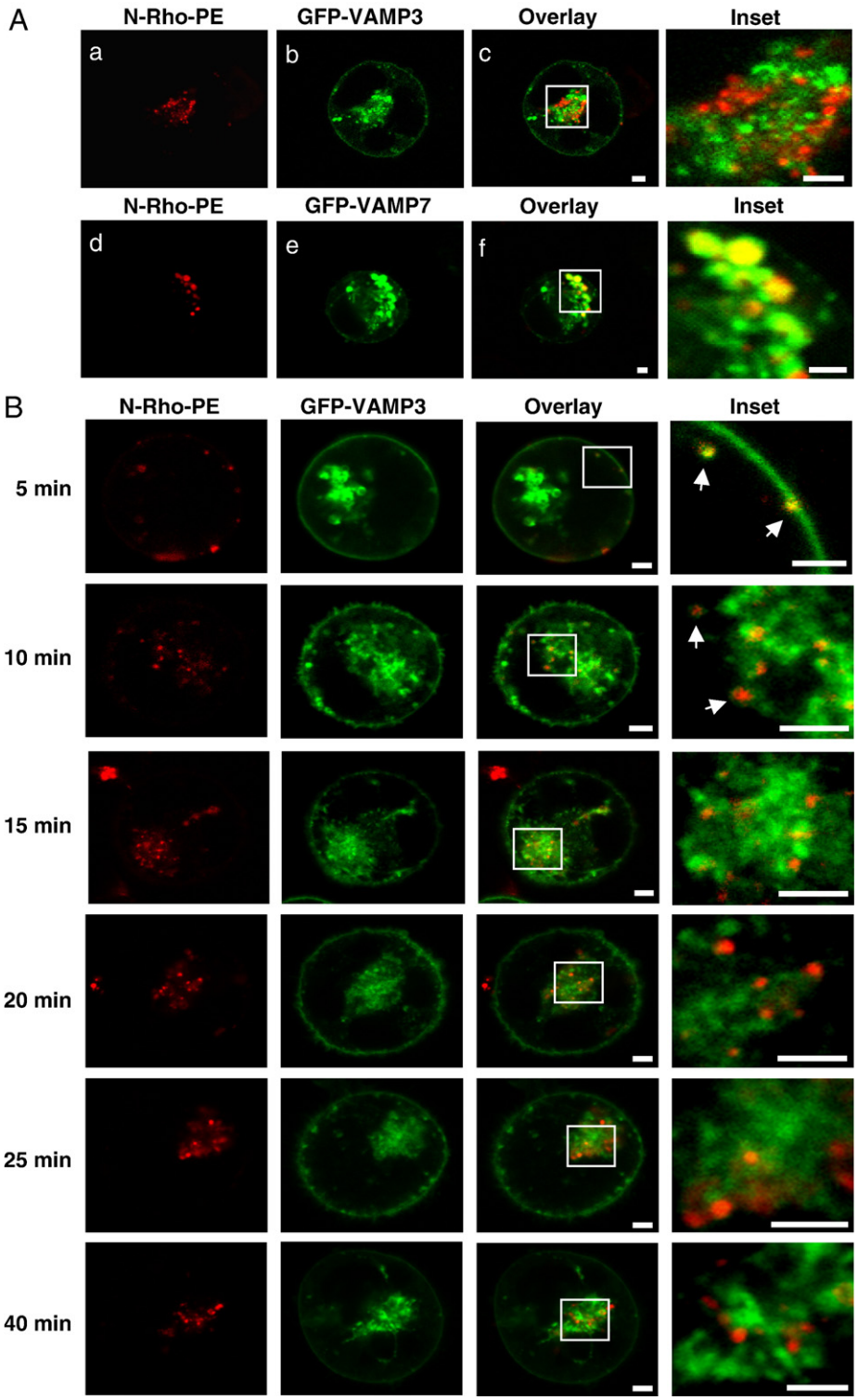

Fig. 1. GFP-VAMP7 decorates large MVBs in K562 cells. (A) K562 cells overexpressing pEGFP-VAMP7 (panels d–f) or pEGFP-VAMP3 (panels a–c) were incubated for 3 h with the fluorescent lipid analog N-Rh-PE to label the MVBs as indicated in Materials and methods. (B) K562 cells overexpressing pEGFP-VAMP3 were incubated for 60 min at 4 °C with N-Rh-PE. Cells were subsequently incubated at 37 °C to allow the internalization of the lipid. At different time points (5, 10, 15, 20, 25, 40 min), the cells were placed on ice and washed with PBS. Cells were mounted on coverslips and immediately analyzed by confocal microscopy. Scale bar: 2 μm.

GFP-VAMP3-labeled vesicular structures were marked with the lipid N-Rh-PE at early times (5 and 10 min) but not at internalization times later than 15–20 min, confirming that in K562 cells VAMP3-labeled vesicles correspond to an early endocytic compartment.

We have previously shown that in K562 cells, GFP-Rab11 decorates a population of MVBs [48,54]. The role of Rab11 in MVB formation was also confirmed in *Drosophila* photoreceptors since Rab11 knockdown led to the generation of abnormal MVBs [55]. To address whether VAMP7 or VAMP3 is present on the Rab11-decorated MVBs, we analyzed these markers in transfected K562 cells overexpressing GFP-Rab11. As shown in Fig. 2, panels a–c, a subset of GFP-Rab11-labeled vesicular structures were marked with the lipid N-Rh-PE, confirming that in K562 cells, MVBs are decorated by Rab11, as previously demonstrated [48]. We next generated double transfectants overexpres-

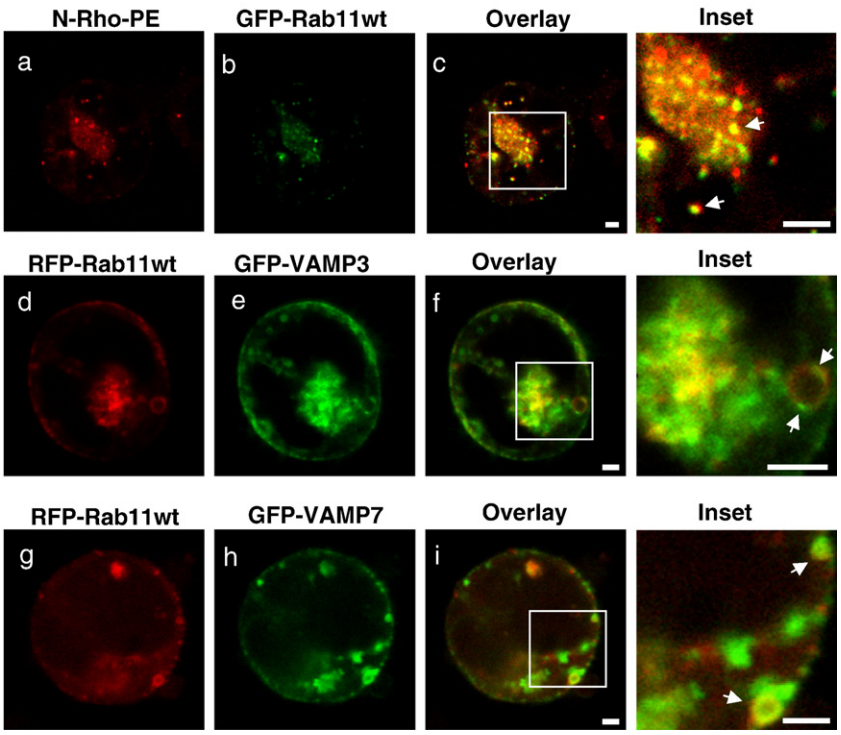

Fig. 2. VAMP3 and VAMP7 colocalize with Rab11-positive vacuoles. K562 cells overexpressing pEGFP-Rab11wt (panels a–c) were incubated for 3 h with the fluorescent lipid analog N-Rh-PE to label the MVBs as indicated in Materials and methods. K562 cells overexpressing RFP-Rab11wt and pEGFP-VAMP3 (panels d–f) or RFP-Rab11wt and pEGFP-VAMP7 (panels g–i) were incubated in full nutrient media. Representative confocal images are depicted. Scale bar: 2 μm.

sing RFP-Rab11 (red) and GFP-VAMP7 (green). As expected, some of the vesicles decorated by Rab11 were also labeled with VAMP7 (Fig. 2, panels g–i). Interestingly, when cells were cotransfected with RFP-Rab11 (red) and GFP-VAMP3 (green), a partial colocalization between Rab11 and VAMP3 was observed (Fig. 2, panels d–f). Our results confirm that VAMP7 decorates MVBs and indicates that a population of vesicles decorated by GFP-Rab11 is VAMP3-positive.

3.2. NH2-terminal domain of VAMP7 causes accumulation of MVBs close to plasma membrane

As mentioned in the Introduction, VAMP7 is involved in constitutive exocytosis in HSY cells [45] and has a possible role for endosomal vesicle trafficking to lysosomes [42,44]. TI-VAMP/VAMP7 has a long N-terminal extension that produces an inhibitory effect on SNARE complex formation [56], and this domain has been used to specifically show the involvement of VAMP7 in a particular vesicular transport event [57,58]. To address whether overexpression of this N-terminal extension of VAMP7, which hampers SNARE pairing, affects the MVBs pathway, we generated transiently transfected K562 cells overexpressing the N-terminal domain of VAMP7 as a fusion protein with GFP (GFP NT-VAMP7) and cells were labeled with the lipid N-Rh-PE (MVB marker). As shown in Fig. 3A, panels a–c, GFP-NT-VAMP7 showed a cytosolic distribution but the punctate pattern of the vesicles labeled with N-Rh-PE was not altered by overexpression of the GFP-NT-VAMP7 domain, indicating that this truncated protein did not affect lipid internalization. However, of note, the N-terminal fragment of VAMP7 generated enlarged MVBs distributed close to the cell periphery, suggesting that a step in the MVB pathway was affected.

Since as indicated above a population of MVBs recruits Rab11 on their limiting membrane, we analyzed the distribution of Rab11 in cells overexpressing both GFP-NT-VAMP7 and RFP-Rab11. As shown in Fig. 3A, panels j–l, numerous Rab11-labeled structures close to plasma membrane were observed. Interestingly, similar to the observed with the lipid, these vesicles presented an enlarged size compared to cells co-expressing RFP-Rab11 and GFP-vector or RFP-Rab11 and GFP-VAMP7, as a control (Fig. 3A, panels d–f and g–i). Since K562 are round cells, the presence of Rab11-positive vesicles close to the cell periphery was confirmed by confocal serial sections (Fig. 3B). The number of enlarged Rab11 vesicles close to the cell surface upon overexpression of NT-VAMP7 was quantified (Fig. 3C), confirming the significant increased percentage of these vesicles close to plasma membrane. In order to verify that overexpression of N-terminal domain of VAMP7 causes enlarged MVBs, a kind of late endosome, to distribute close to the cell periphery, we evaluated the distribution of lysobisphosphatidic acid (LBPA), a late endosome marker, and endogenous VAMP7 in cells overexpressing GFP-vector or GFP-NT-VAMP7. As expected, a population of LBPA-labeled vesicles was clearly decorated by endogenous VAMP7 (Figure S1, panels a–h). On the other hand, cells overexpressing GFP-NT-VAMP7, LBPA-labeled vesicles presented an enlarged size and a nearby plasma membrane distribution compared to cells expressing only GFP (Figure S1, panels e–h). Taken together, these data indicate that overexpression of the NT-domain of VAMP7 leads to a marked increase of enlarged Rab11/N-Rh-PE-marked vesicles (i.e., MVBs) adjacent to the cell periphery, probably by blocking the final fusion step with the plasma membrane.

3.3. MVBs distribution is not affected by inactivating VAMP3

It is known that the light chains of the tetanus (TeNT) and botulinum (BoNTs) neurotoxins have an specific proteotolytic effect (zinc endopeptidases) on certain SNARE proteins [59–61]. The understanding of the biochemical mechanism of action inside neuronal cells has established these toxins as useful tools in studying membrane fusion processes. To date, cellubrevin/VAMP3 is the only known v-SNARE sensitive to tetanus neurotoxin (TeNT) that participates in the endocytic pathway. To address whether inactivation of VAMP3 may also cause an accumulation of MVB close to plasma membrane, K562 cells co-expressing GFP-VAMP3 and the tetanus toxin light chain (pCMV5-TeNT LC) were incubated with the fluorescent lipid analog

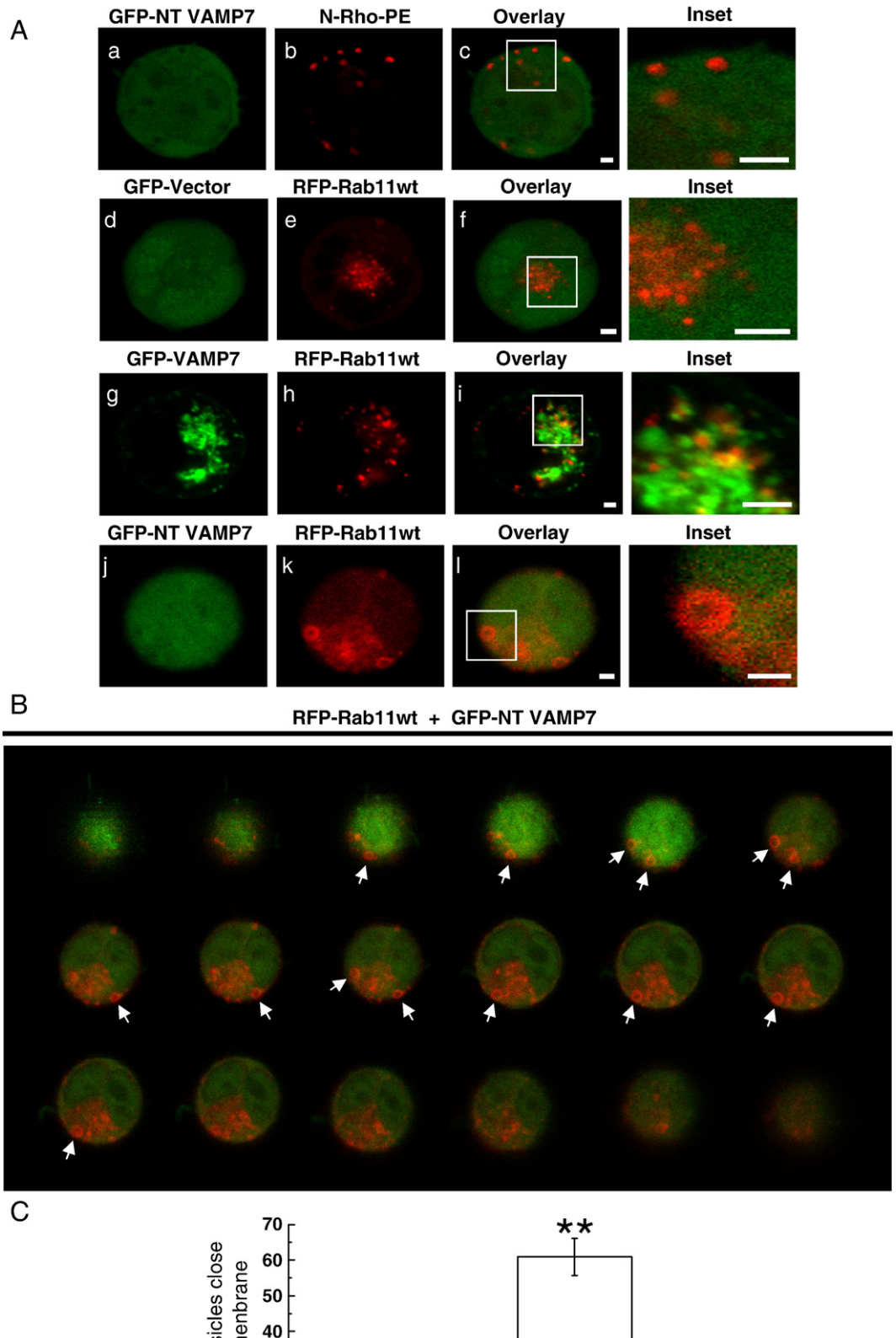
A
GFP-NT VAMP7
N-Rho-PE
Overlay
Inset
a
b
c
GFP-Vector
RFP-Rab11wt
Overlay
Inset
d
e
f
GFP-VAMP7
RFP-Rab11wt
Overlay
Inset
g
h
i
GFP-NT VAMP7
RFP-Rab11wt
Overlay
Inset
j
k
l
B
RFP-Rab11wt + GFP-NT VAMP7
C
% of large vesicles close to plasma menbrane
70
60
50
40
30
20
10
0
**
RFP-Rab11 + GFP-vector
RFP-Rab11 + GFP-NT VAMP7

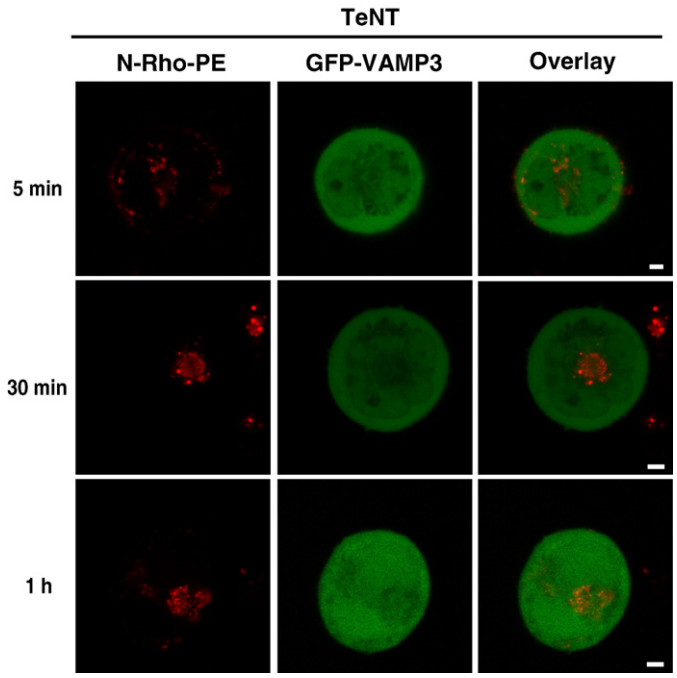

Fig. 4. MVBs distribution is not affected by inactivating VAMP3. K562 cells overexpressing pEGFP-VAMP3 and pCMV5-TeNT were incubated for 60 min at 4 °C with N-Rh-PE. Cells were subsequently incubated at 37 °C to allow the internalization of the lipid. At different time points (5, 30, and 60 min), the cells were placed on ice and washed with PBS. Cells were immediately mounted on coverslips and analyzed by confocal microscopy. Scale bar: 2 μm.

N-Rh-PE. The lipid-labeled structures were analyzed at 5, 30, and 60 min after internalization. As shown in Fig. 4, overexpression of TeNT LC completely changed the distribution of the protein VAMP3 from a vesicular pattern to a soluble distribution. However, VAMP3 inactivation did not affect either the lipid internalization nor the distribution or the size of the MVBs, indicating that VAMP3 does not seem to participate in the biogenesis or exocytosis of the MVBs.

3.4. VAMP7 but not VAMP3 is required for exosome release in K562 cells

It is well known that in K562 cells fusion of MVBs with the plasma membrane results in the release of the internal vesicles known as exosomes into the extracellular medium [6]. As previously shown, the amount of exosomes secreted by these cells can be quantified by measuring the levels of acetylcholinesterase (AChE) [62] in exosome fractions harvested from the culture medium [48]. Since overexpression of NT-VAMP7 caused an accumulation of enlarged MVBs close to the cell periphery, suggesting that fusion with the plasma membrane was abrogated, we were interested in determining if overexpression of VAMP7 affects exosome secretion. After the coupling of v- and t-SNAREs, the chaperone ATPase *N*-ethylmaleimide-sensitive factor (NSF) and soluble NSF attachment proteins (SNAPs) catalyze the disassembly of SNARE complexes, allowing fusion of the transport vesicle with the target membrane [63,64]. Fusion of endosomal vesicles can be readily monitored in vitro and has been shown to require NSF, ATP, and other cytosolic factors [65–67]. Released exosomes were harvested from the culture medium of

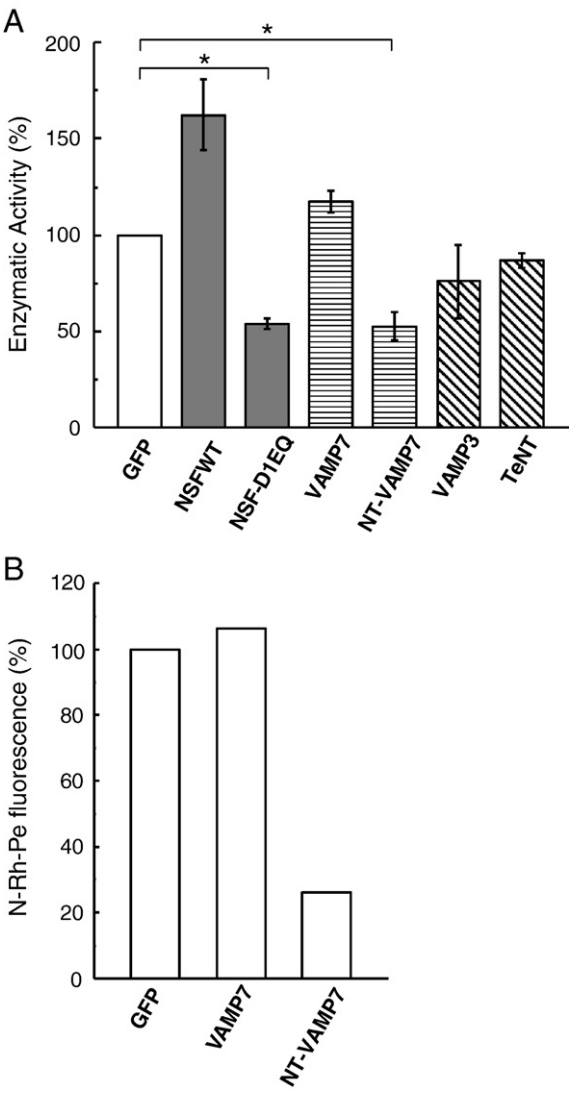

Fig. 5. VAMP7 but not VAMP3 is required for exosome release in K562 cells. (A) Transiently transfected K562 cells overexpressing GFP-vector, GFP-NSF WT, GFP-NSF D1EQ, GFP-VAMP7 WT, GFP-NT-VAMP7, pEGFP-VAMP3, and pcDNA-TeNT LC were incubated for 15 h in full nutrient medium. The released exosomes were collected and quantified by measuring exosome-associated acetylcholinesterase (AChE). Data represent the mean ± SEM of three independent experiments. *Significantly different from the K562 cells transfected with the vector, $P< 0.01$. (B) Cells were labeled for 60 min at 4 °C with the fluorescent lipid analog *N*-(lissamine rhodamine B sulfonyl) phosphatidyl ethanolamine (N-Rh-PE) as described in Materials and methods. Cells were extensively washed with cold PBS to remove excess unbound lipid and were then cultured in complete medium without phenol red to collect exosomes. A sample of the exosomal fraction was suspended in 1.5 ml PBS–TX100 (0.1%), and N-Rh-PE was measured by fluorometry. The figure is representative of two independent experiments.

K562 transfected with GFP-NSF WT (an AAA-ATPase, which is required for recycling and activation of the fusion machinery), GFP-NSF D1EQ (an NSF dominant negative mutant) [68], GFP-VAMP7 WT, GFP-NT-VAMP7, and pcDNA-TeNT LC, and quantified as described under Materials and methods. As shown in Fig. 5A, overexpression of

Fig. 3. Overexpression of NT-VAMP7 causes accumulation of MVBs close to plasma membrane. (A) K562 cells overexpressing pEGFP-VAMP7 (panels a–c) were incubated for 3 h with the fluorescent lipid analog N-Rh-PE to label the MVBs as indicated in Materials and methods. K562 cells overexpressing RFP-Rab11wt and pEGFP-Vector (panels d–f), RFP-Rab11wt, and pGFP-VAMP7 (panels g–i) or RFP-Rab11wt and pEGFP-NT-VAMP7 (panels j–l) were incubated in full nutrient media. Cells were immediately mounted on coverslips and analyzed by confocal microscopy. Scale bar: 2 μm. (B) Serial sections of cells overexpressing RFP-Rab11 (red) and pGFP NT-VAMP7 (green) were obtained by confocal microscopy. Arrows indicate Rab11-positive vesicles close to plasma membrane. (C) Percentage of large vesicles close to plasma membrane in cells overexpressing RFP-Rab11wt and GFP vector or RFP-Rab11wt and pGFP NT-VAMP7 were quantified with the Methamorph software, using the integrated morphometry analysis and represent the mean ± SEM of two independent experiments. At least 100 cells were counted in each condition. **Significantly different from the RFP-Rab11+GFP-vector, $P< 0.005$.

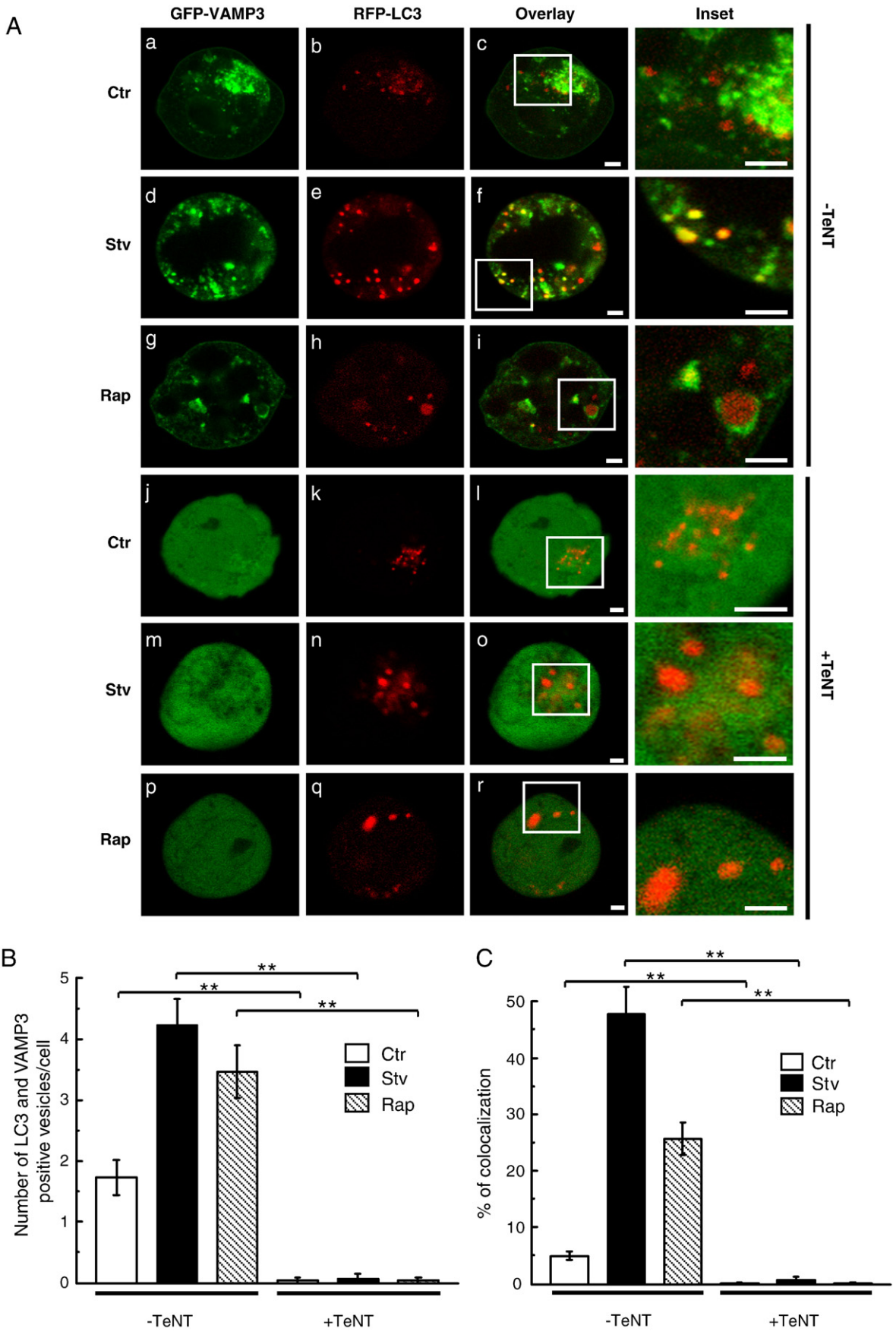
A
GFP-VAMP3
RFP-LC3
Overlay
Inset
Ctr
Stv
Rap
-TeNT
+TeNT
B
Number of LC3 and VAMP3 positive vesicles/cell
Ctr
Stv
Rap
-TeNT
+TeNT
C
% of colocalization
Ctr
Stv
Rap
-TeNT
+TeNT

GFP-NSF WT induced a marked increase in the amount of exosomes released. This effect was abrogated by overexpression of the negative mutant of NSF (GFP-NSF D1EQ). There was a slight increase in the amount of exosomes released by cells overexpressing VAMP7, whereas overexpression of NT-VAMP7 hampered exosome release. Interestingly, no inhibition was observed by expression of the pcDNA-TeNT LC. Similar results were obtained when the exosomes were labeled with the fluorescent lipid analog N-Rh-PE (see Materials and methods). Likewise Fig. 5B shows a marked decrease in the amount of exosomes collected from cells transfected with NT-VAMP7. These results indicate that VAMP7, but not VAMP3, is essential for exosome release in K562 cells. Furthermore, a functional NSF protein is necessary for the process.

3.5. VAMP3 is required for the fusion between autophagosomes and MVBs in K562 cells

Biochemical and morphological studies have shown that autophagosomes can fuse with endosomes forming the so-called amphisomes that are prelysosomal hybrid organelles resulting from the convergence of autophagic/endosomal pathway [69–72]. Interestingly, morphological evidence suggests that MVBs are the main endocytic fusion partners that meet with the autophagosome [18,69]. In a recent publication, we have demonstrated that physiological or pharmacological induction of autophagy markedly increased the interaction between Rab11-decorated MVBs and autophagosomes leading to an enlargement of the hybrid organelle [19].

The protein LC3 is an autophagic marker [73] presents in eukaryotic cells as a soluble form (LC3-I) and a membrane-associated form (LC3-II). LC3-I is conjugated to a lipid molecule to generate LC3-II, which localizes to autophagosomes. To investigate the possible role of VAMP3 in the autophagic pathway, we analyzed this process in transfected K562 cells overexpressing GFP-VAMP3 and RFP-LC3 or GFP-VAMP3, RFP-LC3 and pCMV5-TeNT LC. To activate autophagy, cells were incubated in starvation media or in complete media in the presence of rapamycin, a macrolide antibiotic that stimulates autophagy even under full nutrient conditions by inhibiting the kinase TOR [10]. Interestingly, in cells not expressing the TeNT LC, conditions that trigger autophagy caused a marked increase in the colocalization between LC3 and VAMP3 (Fig. 6A, panels d–f and g–i), compared with the control condition (full nutrient media, panels a–c), as well as an enlargement of the LC3-labeled compartment as previously described [19]. As expected, overexpression of TeNT LC caused the cleavage of the VAMP3 fragment containing the GFP molecule, thus it showed a soluble pattern. However, this VAMP3 cleavage did not affect the enlargement of the LC3-positive vesicles in conditions that stimulate autophagy. The reduction in the amount of VAMP3- and LC3-positive vesicles in K562 overexpressig TeNT LC was quantitated as indicated in Fig. 6B. Likewise, the decreased convergence between VAMP3 and LC3 in the presence of TeNT LC was quantified by measuring the percentage of colocalization between RFP-LC3 and GFP-VAMP3 (Fig. 6C). These results suggest that overexpression of TeNT LC cleavages the protein VAMP3, changing its distribution from a vesicular to a cytosolic pattern, abrogating the colocalization between LC3 and VAMP3 upon autophagy stimulation. However, VAMP3 is not necessary for either the biogenesis or homotypic fusion of the autophagosomes since autophagosomes were formed in cells expressing the toxin that specifically breaks down VAMP3.

To determine whether VAMP3 participates in the fusion between autophagosomes with MVBs to generate the amphisome, we analyzed this process in transfected K562 cells overexpressing GFP-Rab11 and RFP-LC3 or GFP-Rab11 and RFP-LC3 plus pCMV5 TeNT LC. Cells were incubated in starvation media (Fig. 7, panels d–f) or in complete media in the absence (panels a–c) or presence of rapamycin (panels g–i). As expected, conditions that stimulate autophagy caused an increase in the colocalization between LC3 and Rab11 compared with the control condition (Fig. 7, panels f and i). Interestingly, overexpression of the TeNT LC produced a marked decrease in the colocalization between LC3 and Rab11, indicating that fusion between autophagosomes and MVBs was abrogated. The decrease in the number of Rab11- and LC3-positive vesicles in K562 overexpressing TeNT LC was quantified as indicated in Fig. 7B. Also, the decreased percentage of colocalization between GFP-Rab11 and RFP-LC3, in cells overexpressing TeNT LC, was confirmed as indicated in Fig. 7C.

To rule out the possibility that the autophagy-induced enlargement of MVB and the interaction with autophagosomes were due to alterations caused by the overexpression of three chimeric proteins, we analyzed the distribution of endogenous Rab11 and LC3 in cells overexpressing either TeNT LC and RFP-LC3 or GFP-Rab11. Cells were incubated in full nutrient media in the absence (control) or presence of rapamycin (Rap). As shown in Figure S2, panels A and B (see Supplemental Material), in all analyzed cells, the overexpressed proteins and the endogenous proteins (Rab11 or LC3) were targeted to the enlarged vesicles upon autophagy induction and no colocalization was observed in the presence of overexpressed TeNT. Furthermore, the decreased percentage of colocalization between RFP-LC3 and endogenous Rab11 (Figure S2, C left panel) or GFP-Rab11 and endogenous LC3 (Figure S2, C right panel), in cells overexpressing TeNT LC, was confirmed by quantification.

The ability of tetanus neurotoxin to block the interaction between MVBs and autophagosomes was also confirmed by immunoelectron microscopy. Transiently transfected K562 cells overexpressing GFP-LC3 were incubated in complete media (Fig. 8, panel a) or in starvation media in the presence (Fig. 8, panels d–e) or absence (Fig. 8, panels b–c) of TeNT LC and subjected to cryoimmunoelectron microscopy to detect both GFP-LC3 and LBPA, a marker of MVBs. As shown in Fig. 8, in conditions that stimulate autophagy (panels b–c), GFP-LC3 was detected (15-nm gold particles, arrowheads) on the membrane of large vesicles containing small internal vesicles (i.e., MVBs). The internal vesicles were labeled by the anti-LBPA antibody (5-nm gold particles, arrows). GFP labeling correlates to the previously described localization of LC3 both in the outer and inner membranes of autophagosomes [73]. As expected, in control cells (panel a) or in cells incubated under starvation conditions and expressing TeNT LC (panels d–e), only vesicles labeled with GFP-LC3 or LBPA were observed, indicating that under autophagic conditions the tetanus neurotoxin avoids amphisome formation. Taken together, our results suggest that VAMP3 is necessary for the fusion between autophagosomes and MVBs.

3.6. Fusion between autophagosomes and lysosomes is not abrogated by the tetanus toxin

Since as shown in the previous section VAMP3 was required for fusion between autophagosomes and MVBs, we were interested in determining if VAMP3 was involved in fusion among autophagosomes

Fig. 6. Autophagosome formation is not affected by inactivating VAMP3. (A) K562 cells transiently cotransfected with pEGFP-VAMP3 and RFP-LC3 or pEGFP-VAMP3, RFP-LC3 and pcDNA-TeNT LC were incubated for 3 h in full nutrient (Ctr) or amino acid and serum-free media in the absence (Stv) or presence of rapamycin (Rap). Cells were mounted on coverslips and immediately analyzed by confocal microscopy. Scale bar: 2 μm. (B) Number of LC3- and VAMP3-positive vesicles per cell was determined from images as the ones displayed in panel A. (C) Percentage of colocalization between GFP-VAMP3 and RFP-LC3 was also measured. The data were quantified with the Methamorph software, using the integrated morphometry analysis and represent the mean ± SEM of two independent experiments. At least 50 cells were counted in each condition. **Significantly different from the control, $P < 0.005$.

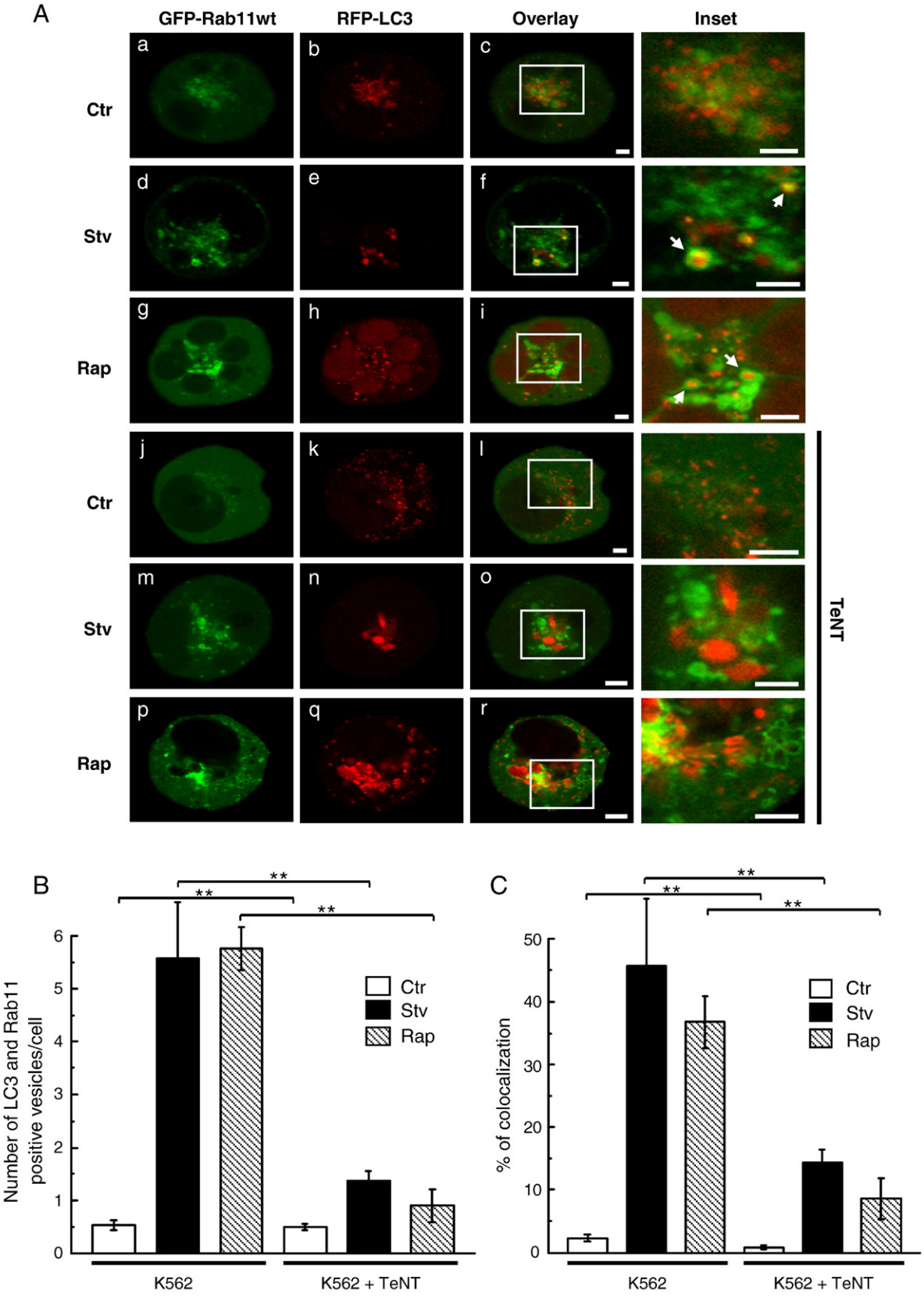

Fig. 7. VAMP3 is required for the fusion between autophagosome and MVBs in K562 cells. K562 cells transiently cotransfected with pEGFP-Rab11wt and RFP-LC3 or pEGFP-Rab11wt, RFP-LC3 and pcDNA-TeNT LC were incubated for 3 h in full nutrient (Ctr) or amino acid and serum-free media in the absence (Stv) or presence of rapamycin (Rap). Cells were mounted on coverslips and immediately analyzed by confocal microscopy. Arrows in the insets indicate LC3 and Rab11 positive amphisomes. Scale bar: 2 μm. (B) Number of LC3 and Rab11-positive vesicles per cell was determined from images as the ones displayed in panel A. (C) Percentage of colocalization between GFP-Rab11 and RFP-LC3 was also measured. The data were quantified with the Methamorph software, using the integrated morphometry analysis and represent the mean ± SEM of three independent experiments. At least 100 cells were counted in each condition. **Significantly different from the control, $P< 0.005$.

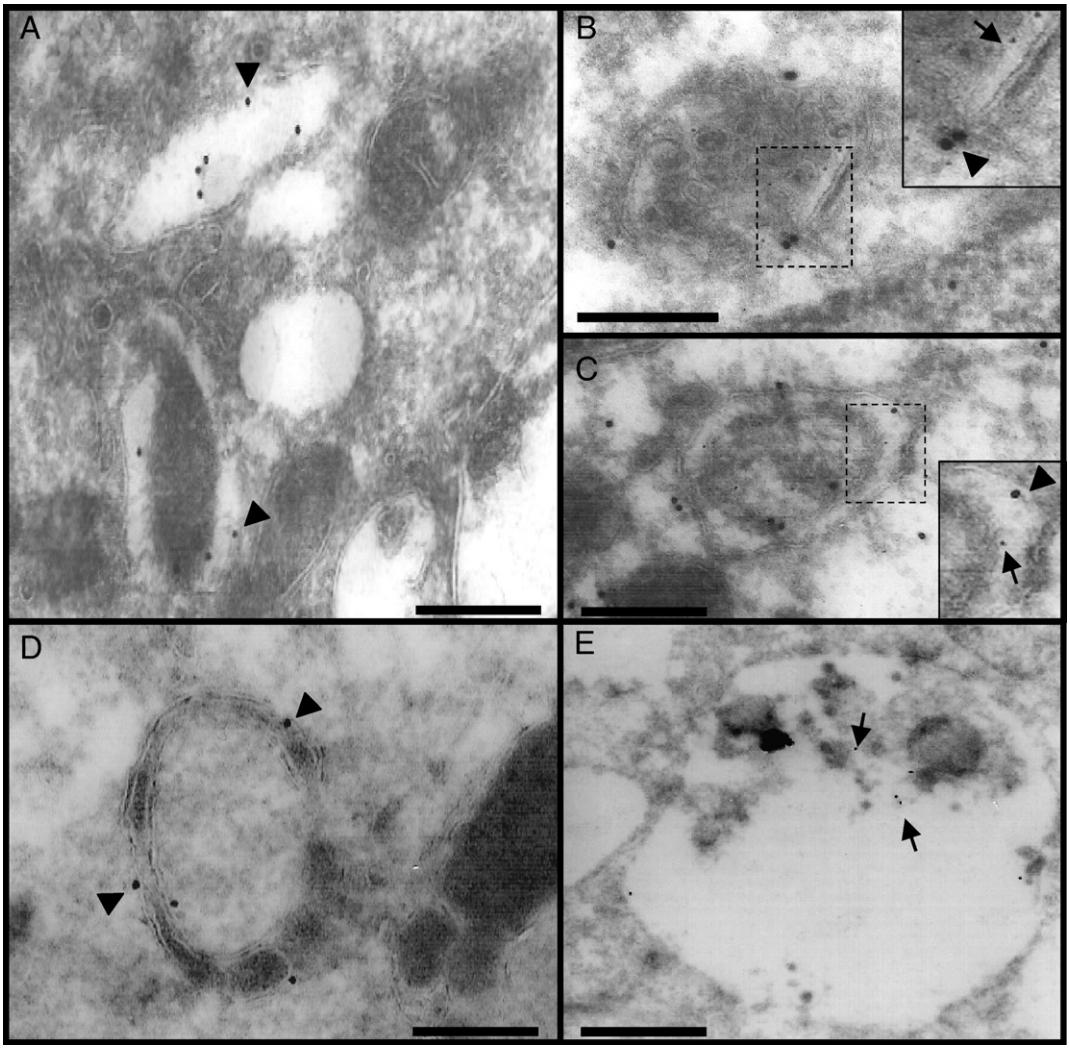

Fig. 8. Immunoelectron microscopy confirm that VAMP3 is present in MVBs and it is required for fusion with autophagosomes. K562 cells overexpressing pGFP-LC3 were incubated for 3 h at 37 °C in full nutrient (a) or amino acid and serum-free media in the absence (b–c) or presence (d–e) of pcDNA-TeNT LC and analyzed by cryoimmunoelectron microscopy. Ultra-thin sections were double labeled with mouse anti-LBPA, followed by a rabbit anti-mouse antibody and rabbit anti-GFP antibody. Rabbit antibodies were detected with protein A coupled to 5-nm or 15-nm gold particles, respectively (see Materials and methods). Arrows: gold particles (protein A gold, 5 nm) detecting LBPA. Arrowheads: gold particles (protein A gold, 15 nm) detecting GFP-LC3. The boxed regions in panels b–c are shown at a higher magnification. Scale bar: 0.5 μm.

and lysosomes. For this purpose, cells were incubated with DQ-BSA for 12 h to label the lysosomal compartment and then transiently cotransfected with GFP-LC3 or GFP-LC3 and TeNT LC. After transfection, cells overexpressing GFP-LC3 were incubated in full nutrient media (Ctr) or in starvation media (Stv). Cells overexpressing GFP-LC3 and TeNT LC were incubated in starvation media (Stv) in the absence or presence of vinblastine (Stv + Vb). Afterwards, cells were incubated with monodansylcadaverine (MDC), an autofluorescent compound that accumulates in autophagic vacuoles [74,75]. As expected, several vesicles were co-labeled with DQ-BSA and the autophagosomal markers GFP-LC3 and MDC in full media (Ctr) or in conditions that stimulate autophagy (Stv) (Fig. 9A, panels a–h). Interestingly, overexpression of TeNT LC did not abrogate the interaction between autophagosomes and lysosomes (Fig. 9A, panels i–l). In contrast, the colocalization between the lysosomal marker (DQ-BSA) and the autophagosomal markers (GFP-LC3 and MDC) was marked inhibited in cells treated with the microtubule-disrupting agent vinblastine (Fig. 9A, panels m–p). The percentage of colocalization between GFP-LC3- and DQ-BSA-positive vesicles in cells overexpressig TeNT LC was quantitated as indicated in Fig. 9B. These results suggest that direct fusion between autophagosomes and lysosomes does not seem to require the v-SNARE protein VAMP3.

3.7. Overexpression of the N-terminal domain of VAMP7 causes a decrease in autolysosome formation

To address whether VAMP7 was involved at some step during the autophagic pathway, we generated transiently transfected K562 cells overexpressing RFP-LC3 and GFP-VAMP7. As shown in Fig. 10A, overexpression of VAMP7 caused an enlargement of vacuoles labeled with LC3 and decorated by VAMP7, indicating that VAMP7 is present in the autophagosomal membrane. Previous works have demonstrated that TI-VAMP/VAMP7 is involved in late endosome to lysosome transport [42,44,58,76]. To investigate the possible role of VAMP7 in the maturation process of the autophagic pathway, K562 cells were transiently transfected with pEGFP-VAMP7 or pEGFP-NT-VAMP7. After 18 h of transfection, cells were incubated with DQ-BSA for 12 h at 37 °C (post-transfection labeling) to label the lysosomal compartment (Fig. 10B, panels a–h). To rule out the possibility that the overexpression of both chimeric proteins can affect the endocytosis of DQ-BSA, a subset of K562 cells were incubated with DQ-BSA for 12 h at 37 °C (pre-transfection labeling) and then cotransfected with pEGFP-VAMP7 or pEGFP-NT-VAMP7 (Fig. 10B, panels i–p) and analyzed after 18 h. Afterwards, cells were incubated with monodansylcadaverine (MDC). As shown in Fig. 10B, overexpression of

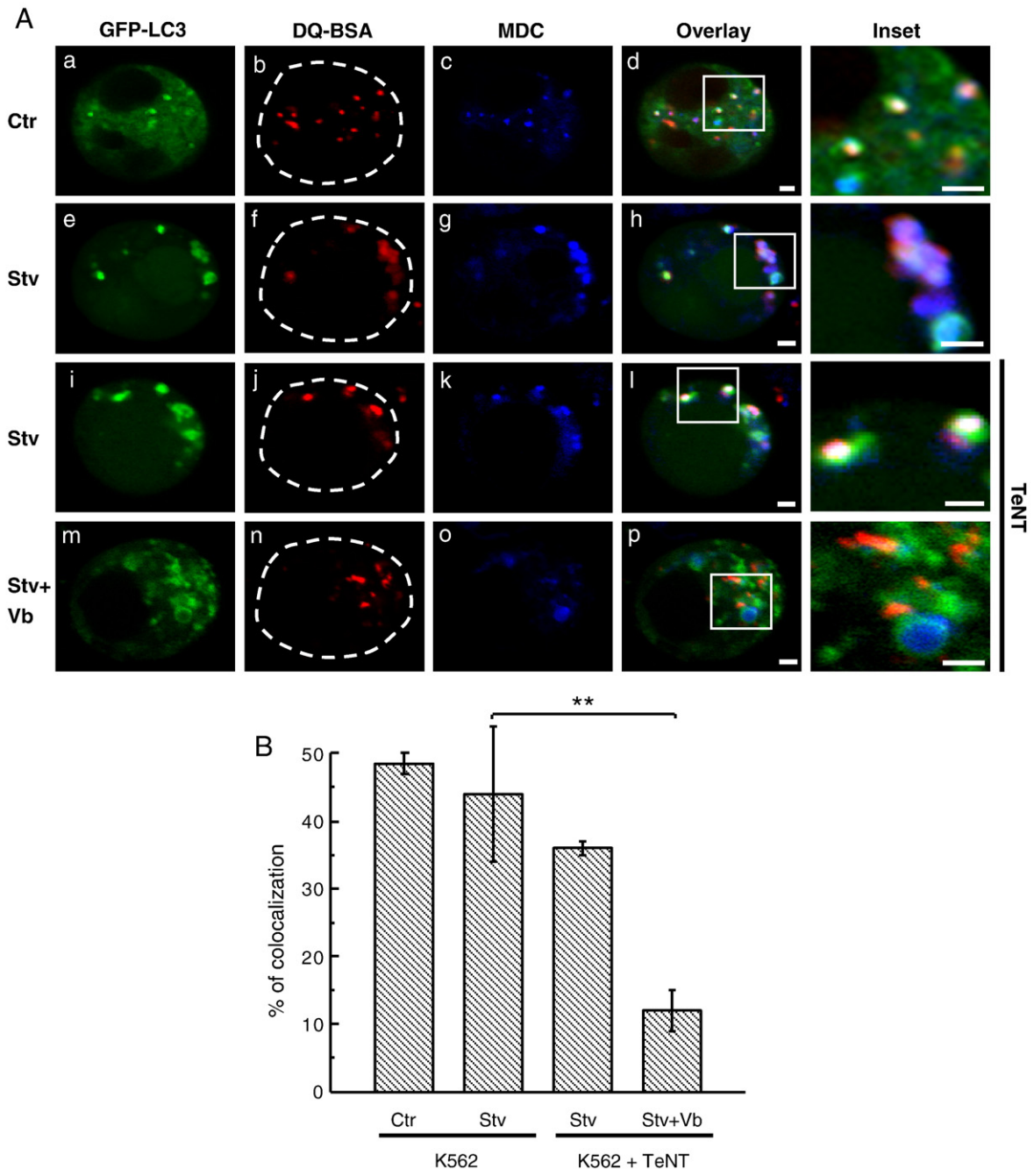

Fig. 9. Direct fusion between autophagosome and lysosome is not abrogated by cleaving VAMP3. (A) K562 cells were incubated with DQ-BSA (10 μg/ml in RPMI + 10% fetal bovine serum) for 12 h at 37 °C to label the lysosomal compartment. Cells were transiently transfected with pEGFP-LC3 or cotransfected with pEGFP-LC3 and pcDNA-TeNT LC. Cells overexpressing pEGFP-LC3 were incubated in full nutrient media (Ctr) or in starvation media (Stv). Cells co-expressing pEGFP-LC3 and pcDNA-TeNT LC were incubated in starvation media (Stv) in the absence or presence of 50 μM of vinblastine (Stv + Vb). Subsequently, cells were incubated with 0.05 mM MDC in PBS at 37 °C for 10 min. After washing several times with cold PBS, cells were mounted on coverslips and immediately analyzed by fluorescence microscopy. Scale bar: 2 μm. (B) Percentage of colocalization between pEGFP-LC3 and DQ-BSA was determined from images as the ones displayed in panel A. The data were quantified with the Methamorph software, using the integrated morphometry analysis and represent the mean ± SEM of three independent experiments. At least 100 cells were counted in each condition. **Significantly different from the control, $P< 0.005$.

GFP-VAMP7 generated some enlarged VAMP7 structures labeled with DQ-BSA and MDC, indicating that these vesicles likely represent autophagolysosomes (panels a–d). As shown before, GFP-NT-VAMP7 showed a cytosolic distribution but the overexpression of NT-VAMP7 caused a marked decrease in DQ-BSA-labeled vesicles compared with untransfected cells (panels e–h, see also Fig. 10C). These data suggest

Fig. 10. Autolysosome formation is abrogated by the overexpression of NT-VAMP7. (A) K562 cells transiently cotransfected with RFP-LC3 and pEGFP-VAMP7 were incubated for 3 h in full nutrient and immediately analyzed by confocal microscopy. (B) K562 cells were transiently transfected with pEGFP-VAMP7 or pEGFP-NT-VAMP7. After 18 h of transfection, cells were incubated with DQ-BSA (10 μg/ml in RPMI + 10% fetal bovine serum) for 12 h at 37 °C to label the lysosomal compartment (panels a–h) (post-transfection labeling). A subset of K562 cells were incubated with DQ-BSA for 12 h at 37 °C. Next, cells were transfected with pEGFP-VAMP7 or pEGFP-NT-VAMP7 (panels i–p) and analyzed after 18 h (pre-transfection labeling). Subsequently, cells were incubated with MDC. After washing several times with cold PBS, cells were mounted on coverslips and immediately analyzed by confocal microscopy. Arrows in the inset indicate autophagosomes. Scale bar: 2 μm. (C) The number of DQ-BSA- and MDC-positive vesicles per cell was determined from images as the ones displayed in panel B. The data were quantified with the Methamorph software, using the integrated morphometry analysis and represent the mean ± SEM of two independent experiments. At least 30 cells were counted in each condition. **Significantly different from the control, $P< 0.005$. *Significantly different from the control, $P< 0.01$.

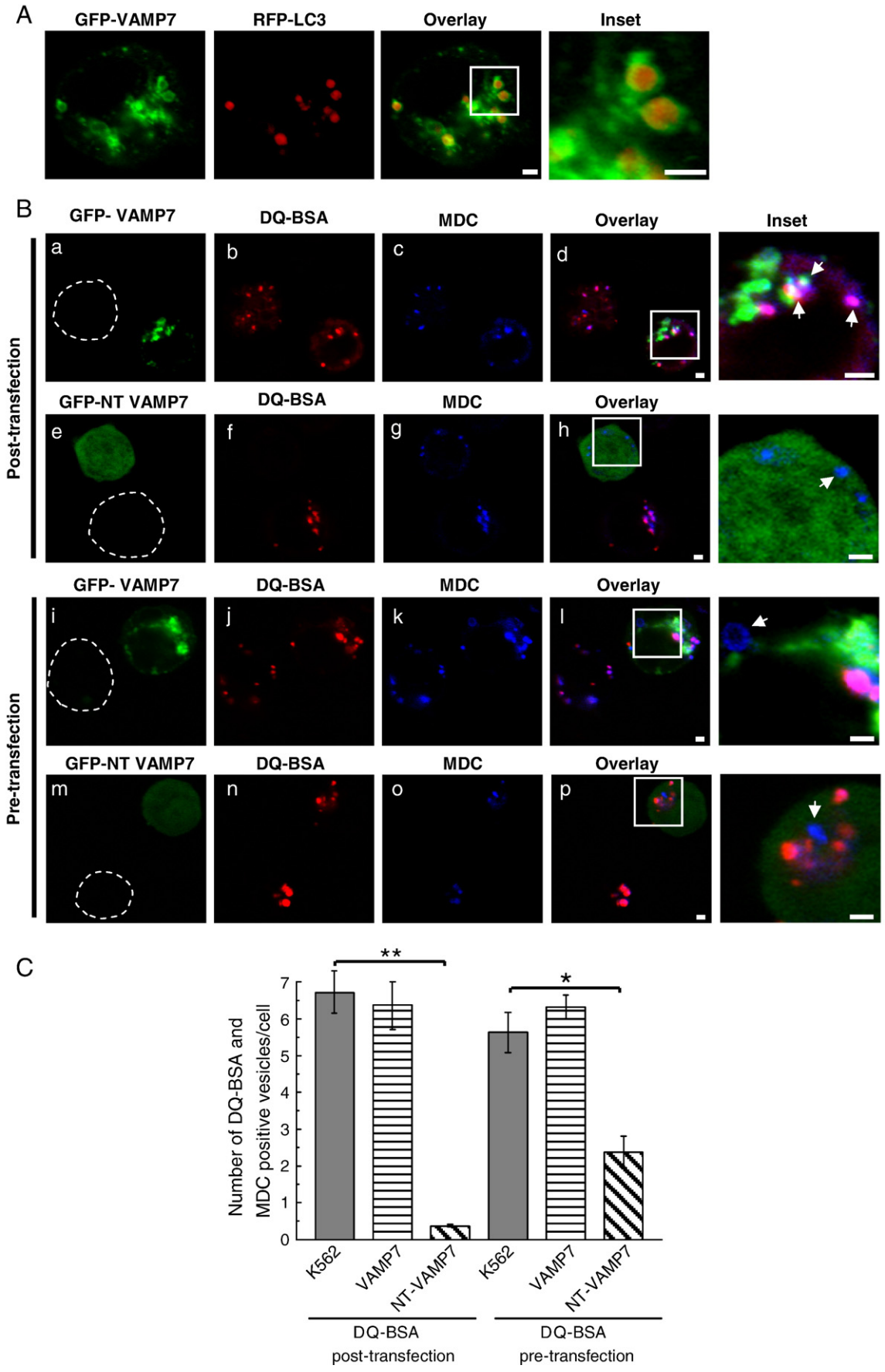
A
GFP-VAMP7
RFP-LC3
Overlay
Inset
B
GFP- VAMP7
DQ-BSA
MDC
Overlay
Inset
Post-transfection
a
b
c
d
GFP-NT VAMP7
DQ-BSA
MDC
Overlay
e
f
g
h
Pre-transfection
GFP- VAMP7
DQ-BSA
MDC
Overlay
i
j
k
l
GFP-NT VAMP7
DQ-BSA
MDC
Overlay
m
n
o
p
C
Number of DQ-BSA and MDC positive vesicles/cell
0
1
2
3
4
5
6
7
**
*
K562
VAMP7
NT-VAMP7
K562
VAMP7
NT-VAMP7
DQ-BSA post-transfection
DQ-BSA pre-transfection

that NT-VAMP7 hampers transport of the endocytosed DQ-BSA to the lysosomal compartment blocking the labeling of degradative structures. Interestingly, in cells pre-labeled with DQ-BSA and then transfected with VAMP7 or NT-VAMP7 (panels i–p), the overexpression of VAMP7 generated enlarged autophagolysosomes labeled with the three markers (GFP-VAMP7, DQ-BSA, and MDC) (panels i–l). In contrast, overexpression of NT-VAMP7 caused a marked decrease in the colocalization between DQ-BSA and MDC. The number of DQ-BSA- and MDC-positive vesicles per cell was quantified as indicated in Fig. 10C, showing the decrease of autolysosomes in cell overexpressing NT-VAMP7. Taken together, these data suggest that NT-VAMP7 blocks autophagosome/lysosome interaction.

4. Discussion

In this study, we have identified two SNARE fusion proteins, TI-VAMP/VAMP7 and VAMP3/cellubrevin that are involved in specific steps of the autophagy /multivesicular body pathways. Several reports have demonstrated that the prototype of the Lodgin subfamily of v-SNARE, TI-VAMP/VAMP7, participates in trafficking events [35,44,77]. TI-VAMP/VAMP7 was proposed to mediate late endosome to lysosome transport [58]. In this report, we present evidence that in K562 cells TI-VAMP/VAMP7 but not VAMP3 participates in the fusion between MVBs with the plasma membrane. Our results indicate that enlarged MVBs (decorated with GFP-Rab11 and labeled by the lipid N-Rh-PE) colocalize with the overexpressed GFP-TI-VAMP/VAMP7. Likewise, we show that endogenous VAMP7 protein is overlapped in enlarged LBPA (late endosome/MVB marker) vesicles. This observation is consistent with previous reports showing that TI-VAMP/VAMP7 colocalizes with CD63, a marker of MVB late endosomes, in PC12 and HeLa cells [50,78]. Moreover, L1 (a cell–cell adhesion molecule), which colocalized with TI-VAMP in the developing brain, was also found in the internal vesicles of MVB [50,51,79]. Furthermore, we have also observed that overexpression of the N-terminal domain of TI-VAMP/VAMP7, which inhibits SNARE complex formation [80], caused an enlargement of the MVB, which were distributed at the cell periphery, suggesting that an active TI-VAMP/VAMP7 is necessary for fusion of MVBs with the plasma membrane. Interestingly, the punctate distribution of the MVB labeled with N-Rh-PE was not affected by overexpression of the GFP-NT-TI-VAMP/VAMP7 mutant, which remained in a vesicular-like pattern, indicating that this mutant did not affect either lipid internalization or MVBs biogenesis. Similar results were obtained in MDCK cells where the overexpression of NT VAMP7 slowed down endocytosis, but this process was not abrogated [52]. On the other hand, we have observed that overexpression of TI-VAMP leads to clear inhibition (approximately 90%) of the labeling of vesicles when DQ-BSA was internalized after transfection of GFP-NT VAMP7. In addition, there was a marked decrease in the colocalization between autophagic and lysosomal markers when the cells were pre-labeled with DQ-BSA and then transfected with the N-terminal domain of TI-VAMP. These data are consistent with the observation that VAMP7 is involved in the late endosome to lysosome transport [42,44,58,76] and that overexpression of TI-VAMP impairs this endocytic step. Likewise, overexpression of TI-VAMP hampered lysosomal secretion perhaps because it affects the biogenesis of the late endosomal and lysosomal compartments [52].

We have previously shown that in K562 cells, GFP-Rab11 and also the endogenous protein decorate a population of MVBs [19,48,54]. Furthermore, Rab11 has been detected by proteomics in exosomes, the internal vesicles released by a type of MVBs [81]. Moreover, a role for Rab11 in the formation of MVBs in *Drosophila melanogaster* was also demonstrated [55]. Interestingly, we observed that TI-VAMP/VAMP7 colocalized with enlarged Rab11 vesicles, indicating that TI-VAMP/VAMP7 is present in at least a subset of MVBs. Likewise, the overexpression of the N-terminal domain of TI-VAMP/VAMP7 caused an accumulation of Rab11 vesicles distributed at the cell periphery, suggesting that TI-VAMP/VAMP7 is necessary for the fusion of MVB with plasma membrane to release the exosomes. In addition consistent with this observation, we have observed that overexpression of NT-TI-VAMP/VAMP7 markedly decreased exosome release. This is in agreement with the results obtained in Therry Gally's laboratory where they demonstrated that the overexpression of the N-terminal domain of TI-VAMP/VAMP7 abrogated lysosomal secretion and consequently membrane repair [52].

VAMP3/cellubrevin has been postulated to function as a v-SNARE for early and recycling endosomes and probably for constitutive exocytosis [82]. This protein has a central conserved domain at the cytoplasmic side, which contains the cleavage site for TeNT, being VAMP3 sensitive to the proteolytic effect of this toxin. Overexpression of pcDNA LC-TeTN caused a dramatic change in the distribution of GFP-VAMP3, which remained cytosolic, indicating that VAMP3 was effectively cleaved by TeNT, leaving the GFP-NH2 terminal fragment of this protein soluble in the cytosol. This observation is consistent with previous reports that have shown that TeNT breaks down VAMP3 in a selective manner [83]. Interestingly, our results indicate that MVBs biogenesis was not affected by the proteolytic effect of TeNT on VAMP3 and overexpression of VAMP3 or tetanus toxin did not affect the amount of exosome released, suggesting that this protein does not have a critical role in these steps of the MBV pathway.

Several studies have shown the convergence of the autophagic/endosomal pathways in different cell types [69–72]. Moreover, we have verified that physiological or pharmacological induction of autophagy markedly increased the interaction between MVBs and autophagosomes leading to enlarged amphisomes [19]. In the present report, we demonstrate that VAMP3 colocalizes with autophagic vacuoles under conditions that stimulate autophagy, being this colocalization hampered by TeNT. In contrast, TeNT did not block the enlargement of the autophagosomes due to autophagy stimulation, indicating that VAMP3 is not necessary for the biogenesis of the autophagosome. In addition, we have observed that a subset of VAMP3-positive vacuoles colocalize with Rab11. These data are consistent with the fact that Rab11 decorates the membrane of autophagic vacuoles (amphisomes) in K562 cells [19], being necessary for amphisome formation. Interestingly, we have demonstrated by immunofluorescence and ultrastructural analysis that in K562 cells TeNT inhibited the interaction between Rab11-decorated MVBs and autophagosomes. These results indicate that VAMP3 is required for the fusion between MVBs with autophagosomes, allowing the maturation of the autophagic vacuole.

Previous studies have shown that the effect of vinblastine within the autophagic pathway is likely due to inhibition of fusion of autophagosomes and amphisomes with lysosomes, without affecting autophagosome–amphisome fusion [69,71]. In a previous report, we have indeed demonstrated that the interaction between MVBs and autophagic vacuoles was not prevented when microtubules were disrupted by vinblastine [19]. Importantly, our results show that TeNT did not hamper the formation of the autolysosome, which was only blocked when cells were incubated in the presence of the microtubule inhibitor vinblastine. These data suggest that VAMP3 is required for amphisome generation but it is not required for direct fusion between autophagosomes and lysosomes.

During reticulocyte maturation, hematopoietic progenitors undergo numerous changes to reach the final functional stage, the erythrocyte. Throughout this process, some proteins and organelles that are not required in the mature red cell are lost. These proteins are released into the extracellular medium associated with vesicles present in multivesicular bodies (MVBs) [3,4,6–8,84]. In addition, in the transformation process that occurs during erythrocyte maturation, intracellular organelles are likely removed by means of autophagic sequestration and degradation. Genetic evidence has

been recently provided indicating that autophagy is involved in mitochondrial clearance from reticulocytes [85]. Likewise, it has been previously demonstrated that Ulk1 (homologue to the yeast autophagy kinase Atg1) is a critical regulator of mitochondrial and ribosomal clearance during erythroid maturation [86]. We have also demonstrated that in the erithroleukemic K562 cells, MVBs interact with the autophagic pathway and that autophagy likely contributes to get rid of these endocytic compartments in this cell type [19]. In the present report, we have presented evidence indicating the role of two SNAREs proteins (VAMP7 and VAMP3) in specific steps of the MVB/autophagic pathway. We believe that our study opens a new avenue to unravel the biological significance of autophagy in a physiological process such as the terminal differentiation of red blood cells.

Acknowledgements

We thank Cecilia Lerena and Cristina Vázquez, members of the laboratory, for critical reading of this manuscript. We also thank Alejandra Medero for technical assistance with tissue culture. This work was partly supported by grants from Agencia Nacional de Promoción Científica y Tecnológica (PICT 2004 20711 and PICT 2005 38420), Secyt (Universidad Nacional de Cuyo) to M.I.C.

Appendix A. Supplementary data

Supplementary data associated with this article can be found, in the online version, at doi:10.1016/j.bbamcr.2009.09.011.

References

[1] R.M. Johnstone, M. Adam, J.R. Hammond, L. Orr, C. Turbide, Vesicle formation during reticulocyte maturation. Association of plasma membrane activities with released vesicles (exosomes), J. Biol. Chem. 262 (1987) 9412–9420.
[2] B.B. Lozzio, C.B. Lozzio, E.G. Bamberger, A.S. Feliu, A multipotential leukemia cell line (K-562) of human origin, Proc. Soc. Exp. Biol. Med. 166 (1981) 546–550.
[3] C. Harding, J. Heuser, P. Stahl, Endocytosis and intracellular processing of transferrin and colloidal gold-transferrin in rat reticulocytes: demonstration of a pathway for receptor shedding, Eur. J. Cell Biol. 35 (1984) 256–263.
[4] R.M. Johnstone, A. Mathew, A.B. Mason, K. Teng, Exosome formation during maturation of mammalian and avian reticulocytes: evidence that exosome release is a major route for externalization of obsolete membrane proteins, J. Cell Physiol. 147 (1991) 27–36.
[5] R.M. Johnstone, The Jeanne Manery-Fisher Memorial Lecture, Maturation of reticulocytes: formation of exosomes as a mechanism for shedding membrane proteins, Biochem. Cell Biol. 70 (1992) (1991) 179–190.
[6] R.M. Johnstone, Cleavage of the transferrin receptor by human granulocytes: differential proteolysis of the exosome-bound TFR, J. Cell Physiol. 168 (1996) 333–345.
[7] G. Raposo, H.W. Nijman, W. Stoorvogel, R. Liejendekker, C.V. Harding, C.J. Melief, H.J. Geuze, B lymphocytes secrete antigen-presenting vesicles, J. Exp. Med. 183 (1996) 1161–1172.
[8] C. Thery, L. Zitvogel, S. Amigorena, Exosomes: composition, biogenesis and function. Nat. Rev. Immunol. 2 (8) (2002) 569–579 Ref Type: Generic.
[9] W.A. Dunn, Studies on the mechanisms of autophagy: formation of the autophagic vacuole, J. Cell Biol. 110 (1990) 1923–1933.
[10] D.J. Klionsky, S.D. Emr, Autophagy as a regulated pathway of cellular degradation, Science 290 (2000) 1717–1721.
[11] G.E. Mortimore, A.R. Poso, The lysosomal pathway of intracellular proteolysis in liver: regulation by amino acids, Adv. Enzyme Regul. 25 (1986) 257–276.
[12] G.E. Mortimore, B.R. Lardeux, S.J. Heydrick, Mechanism and control of protein and RNA degradation in the rat hepatocyte: two modes of autophagic sequestration, Revis. Biol. Celular. 20 (1989) 79–96.
[13] P.O. Seglen, P.B. Gordon, I. Holen, H. Hoyvik, Hepatocytic autophagy, Biomed. Biochim. Acta 50 (1991) 373–381.
[14] M.J. Heynen, G. Tricot, R.L. Verwilghen, Autophagy of mitochondria in rat bone marrow erythroid cells. Relation to nuclear extrusion, Cell Tissue Res. 239 (1985) 235–239.
[15] G. Kent, O.T. Minick, F.I. Volini, E. Orfei, Autophagic vacuoles in human red cells, Am. J. Pathol. 48 (1966) 831–857.
[16] H. Takano-Ohmuro, M. Mukaida, E. Kominami, K. Morioka, Autophagy in embryonic erythroid cells: its role in maturation, Eur. J. Cell Biol. 79 (2000) 759–764.
[17] T. Shintani, D.J. Klionsky, Autophagy in health and disease: a double-edged sword, Science 306 (2004) 990–995.
[18] J. Yi, X.M. Tang, The convergent point of the endocytic and autophagic pathways in Leydig cells, Cell Res. 9 (1999) 243–253.
[19] C.M. Fader, D. Sanchez, M. Furlan, M.I. Colombo, Induction of autophagy promotes fusion of multivesicular bodies with autophagic vacuoles in k562 cells, Traffic 9 (2008) 230–250.
[20] J. Morvan, R. Kochl, R. Watson, L.M. Collinson, H.B. Jefferies, S.A. Tooze, In vitro reconstitution of fusion between immature autophagosomes and endosomes, Autophagy 5 (2009) 676–689.
[21] M. Babst, D.J. Katzmann, W.B. Snyder, B. Wendland, S.D. Emr, Endosome-associated complex, ESCRT-II, recruits transport machinery for protein sorting at the multivesicular body, Dev. Cell 3 (2002) 283–289.
[22] M. Babst, D.J. Katzmann, E.J. Estepa-Sabal, T. Meerloo, S.D. Emr, Escrt-III: an endosome-associated heterooligomeric protein complex required for mvb sorting, Dev. Cell 3 (2002) 271–282.
[23] M. Babst, A protein's final ESCRT, Traffic 6 (2005) 2–9.
[24] D.J. Katzmann, M. Babst, S.D. Emr, Ubiquitin-dependent sorting into the multivesicular body pathway requires the function of a conserved endosomal protein sorting complex, ESCRT-I, Cell 106 (2001) 145–155.
[25] K.G. Bache, A. Brech, A. Mehlum, H. Stenmark, Hrs regulates multivesicular body formation via ESCRT recruitment to endosomes, J. Cell Biol. 162 (2003) 435–442.
[26] P.S. Bilodeau, J.L. Urbanowski, S.C. Winistorfer, R.C. Piper, The Vps27p Hse1p complex binds ubiquitin and mediates endosomal protein sorting, Nat. Cell Biol. 4 (2002) 534–539.
[27] C. Raiborg, H. Stenmark, Hrs and endocytic sorting of ubiquitinated membrane proteins, Cell Struct. Funct. 27 (2002) 403–408.
[28] S.C. Shih, D.J. Katzmann, J.D. Schnell, M. Sutanto, S.D. Emr, L. Hicke, Epsins and Vps27p/Hrs contain ubiquitin-binding domains that function in receptor endocytosis, Nat. Cell Biol. 4 (2002) 389–393.
[29] K.A. Swanson, R.S. Kang, S.D. Stamenova, L. Hicke, I. Radhakrishnan, Solution structure of Vps27 UIM–ubiquitin complex important for endosomal sorting and receptor downregulation, EMBO J. 22 (2003) 4597–4606.
[30] M. Filimonenko, S. Stuffers, C. Raiborg, A. Yamamoto, L. Malerod, E.M. Fisher, A. Isaacs, A. Brech, H. Stenmark, A. Simonsen, Functional multivesicular bodies are required for autophagic clearance of protein aggregates associated with neurodegenerative disease, J. Cell Biol. 179 (2007) 485–500.
[31] J.A. Lee, A. Beigneux, S.T. Ahmad, S.G. Young, F.B. Gao, ESCRT-III dysfunction causes autophagosome accumulation and neurodegeneration, Curr. Biol. 17 (2007) 1561–1567.
[32] C.M. Fader, M.I. Colombo, Autophagy and multivesicular bodies: two closely related partners, Cell Death Differ. (2008).
[33] T.E. Rusten, A. Simonsen, ESCRT functions in autophagy and associated disease, Cell Cycle (2008) 7.
[34] S. Martens, H.T. McMahon, Mechanisms of membrane fusion: disparate players and common principles, Nat. Rev. Mol. Cell Biol. 9 (2008) 543–556.
[35] W. Antonin, D. Fasshauer, S. Becker, R. Jahn, T.R. Schneider, Crystal structure of the endosomal SNARE complex reveals common structural principles of all SNAREs, Nat. Struct. Biol. 9 (2002) 107–111.
[36] R.B. Sutton, D. Fasshauer, R. Jahn, A.T. Brunger, Crystal structure of a SNARE complex involved in synaptic exocytosis at 2.4 A resolution, Nature 395 (1998) 347–353.
[37] R. Jahn, T.C. Sudhof, Membrane fusion and exocytosis, Annu. Rev. Biochem. 68 (1999) 863–911.
[38] L. Johannes, T. Galli, Exocytosis: SNAREs drum up! Eur. J. Neurosci. 10 (1998) 415–422.
[39] G. hnert-Hilger, U. Kutay, I. Chahoud, T. Rapoport, B. Wiedenmann, Synaptobrevin is essential for secretion but not for the development of synaptic processes, Eur. J. Cell Biol. 70 (1996) 1–11.
[40] A. Osen-Sand, J.K. Staple, E. Naldi, G. Schiavo, O. Rossetto, S. Petitpierre, A. Malgaroli, C. Montecucco, S. Catsicas, Common and distinct fusion proteins in axonal growth and transmitter release, J. Comp Neurol. 367 (1996) 222–234.
[41] T. Galli, A. Zahraoui, V.V. Vaidyanathan, G. Raposo, J.M. Tian, M. Karin, H. Niemann, D. Louvard, A novel tetanus neurotoxin-insensitive vesicle-associated membrane protein in SNARE complexes of the apical plasma membrane of epithelial cells, Mol. Biol. Cell 9 (1998) 1437–1448.
[42] R.J. Advani, H.R. Bae, J.B. Bock, D.S. Chao, Y.C. Doung, R. Prekeris, J.S. Yoo, R.H. Scheller, Seven novel mammalian SNARE proteins localize to distinct membrane compartments, J. Biol. Chem. 273 (1998) 10317–10324.
[43] S. Martinez-Arca, P. Alberts, T. Galli, Clostridial neurotoxin-insensitive vesicular SNAREs in exocytosis and endocytosis, Biol. Cell 92 (2000) 449–453.
[44] R.J. Advani, B. Yang, R. Prekeris, K.C. Lee, J. Klumperman, R.H. Scheller, VAMP-7 mediates vesicular transport from endosomes to lysosomes, J. Cell Biol. 146 (1999) 765–776.
[45] Y. Oishi, T. Arakawa, A. Tanimura, M. Itakura, M. Takahashi, Y. Tajima, I. Mizoguchi, T. Takuma, Role of VAMP-2, VAMP-7, and VAMP-8 in constitutive exocytosis from HSY cells, Histochem, Cell Biol. 125 (2006) 273–281.
[46] C.C. Wang, C.P. Ng, L. Lu, V. Atlashkin, W. Zhang, L.F. Seet, W. Hong, A role of VAMP8/endobrevin in regulated exocytosis of pancreatic acinar cells, Dev. Cell 7 (2004) 359–371.
[47] C. Yang, S. Mora, J.W. Ryder, K.J. Coker, P. Hansen, L.A. Allen, J.E. Pessin, VAMP3 null mice display normal constitutive, insulin- and exercise-regulated vesicle trafficking, Mol. Cell Biol. 21 (2001) 1573–1580.
[48] A. Savina, M. Vidal, M.I. Colombo, The exosome pathway in K562 cells is regulated by Rab11, J. Cell Sci. 115 (2002) 2505–2515.
[49] S. Breton, N.N. Nsumu, T. Galli, I. Sabolic, P.J. Smith, D. Brown, Tetanus toxin-mediated cleavage of cellubrevin inhibits proton secretion in the male reproductive tract, Am. J. Physiol. Renal Physiol. 278 (2000) F717–F725.
[50] S. Martinez-Arca, R. Rudge, M. Vacca, G. Raposo, J. Camonis, V. Proux-Gillardeaux, L. Daviet, E. Formstecher, A. Hamburger, F. Filippini, M. D'Esposito, T. Galli, A dual

mechanism controlling the localization and function of exocytic v-SNAREs, Proc. Natl. Acad. Sci. U. S. A 100 (2003) 9011–9016.
[51] V. Proux-Gillardeaux, R. Rudge, T. Galli, The tetanus neurotoxin-sensitive and insensitive routes to and from the plasma membrane: fast and slow pathways? Traffic 6 (2005) 366–373.
[52] V. Proux-Gillardeaux, G. Raposo, T. Irinopoulou, T. Galli, Expression of the Longin domain of TI-VAMP impairs lysosomal secretion and epithelial cell migration, Biol. Cell 99 (2007) 261–271.
[53] M. Vidal, P. Mangeat, D. Hoekstra, Aggregation reroutes molecules from a recycling to a vesicle-mediated secretion pathway during reticulocyte maturation, J. Cell Sci. 110 (Pt. 16) (1997) 1867–1877.
[54] A. Savina, C.M. Fader, M.T. Damiani, M.I. Colombo, Rab11 promotes docking and fusion of multivesicular bodies in a calcium-dependent manner, Traffic 6 (2005) 131–143.
[55] A.K. Satoh, J.E. O'Tousa, K. Ozaki, D.F. Ready, Rab11 mediates post-Golgi trafficking of rhodopsin to the photosensitive apical membrane of *Drosophila* photoreceptors, Development 132 (2005) 1487–1497.
[56] S. Martinez-Arca, P. Alberts, A. Zahraoui, D. Louvard, T. Galli, Role of tetanus neurotoxin insensitive vesicle-associated membrane protein (TI-VAMP) in vesicular transport mediating neurite outgrowth, J. Cell Biol. 149 (2000) 889–900.
[57] V. Braun, V. Fraisier, G. Raposo, I. Hurbain, J.B. Sibarita, P. Chavrier, T. Galli, F. Niedergang, TI-VAMP/VAMP7 is required for optimal phagocytosis of opsonised particles in macrophages, EMBO J. 23 (2004) 4166–4176.
[58] P.R. Pryor, B.M. Mullock, N.A. Bright, M.R. Lindsay, S.R. Gray, S.C. Richardson, A. Stewart, D.E. James, R.C. Piper, J.P. Luzio, Combinatorial SNARE complexes with VAMP7 or VAMP8 define different late endocytic fusion events, EMBO Rep. 5 (2004) 590–595.
[59] Y. Humeau, F. Doussau, N.J. Grant, B. Poulain, How botulinum and tetanus neurotoxins block neurotransmitter release, Biochimie 82 (2000) 427–446.
[60] G. Schiavo, M. Matteoli, C. Montecucco, Neurotoxins affecting neuroexocytosis, Physiol. Rev. 80 (2000) 717–766.
[61] K. Turton, J.A. Chaddock, K.R. Acharya, Botulinum and tetanus neurotoxins: structure, function and therapeutic utility, Trends Biochem. Sci. 27 (2002) 552–558.
[62] R.M. Johnstone, A. Bianchini, K. Teng, Reticulocyte maturation and exosome release: transferrin receptor containing exosomes shows multiple plasma membrane functions, Blood 74 (1989) 1844–1851.
[63] D.O. Clary, I.C. Griff, J.E. Rothman, SNAPs, a family of NSF attachment proteins involved in intracellular membrane fusion in animals and yeast, Cell 61 (1990) 709–721.
[64] T. Sollner, M.K. Bennett, S.W. Whiteheart, R.H. Scheller, J.E. Rothman, A protein assembly-disassembly pathway in vitro that may correspond to sequential steps of synaptic vesicle docking, activation, and fusion, Cell 75 (1993) 409–418.
[65] W.A. Braell, Fusion between endocytic vesicles in a cell-free system, Proc. Natl. Acad. Sci. U. S. A. 84 (1987) 1137–1141.
[66] M.I. Colombo, Role for NSF on vesicular transport: insights from in vitro endosome fusion, Biocell 20 (1996) 317–323.
[67] J.P. Gorvel, P. Chavrier, M. Zerial, J. Gruenberg, rab5 controls early endosome fusion in vitro, Cell 64 (1991) 915–925.
[68] S.W. Whiteheart, K. Rossnagel, S.A. Buhrow, M. Brunner, R. Jaenicke, J.E. Rothman, *N*-ethylmaleimide-sensitive fusion protein: a trimeric ATPase whose hydrolysis of ATP is required for membrane fusion, J. Cell Biol. 126 (1994) 945–954.
[69] T.O. Berg, M. Fengsrud, P.E. Stromhaug, T. Berg, P.O. Seglen, Isolation and characterization of rat liver amphisomes. Evidence for fusion of autophagosomes with both early and late endosomes, J. Biol. Chem. 273 (1998) 21883–21892.
[70] P.B. Gordon, P.O. Seglen, Prelysosomal convergence of autophagic and endocytic pathways, Biochem. Biophys. Res. Commun. 151 (1988) 40–47.
[71] P.B. Gordon, H. Hoyvik, P.O. Seglen, Prelysosomal and lysosomal connections between autophagy and endocytosis, Biochem. J. 283 (Pt. 2) (1992) 361–369.
[72] J. Tooze, M. Hollinshead, T. Ludwig, K. Howell, B. Hoflack, H. Kern, In exocrine pancreas, the basolateral endocytic pathway converges with the autophagic pathway immediately after the early endosome, J. Cell Biol. 111 (1990) 329–345.
[73] Y. Kabeya, N. Mizushima, T. Ueno, A. Yamamoto, T. Kirisako, T. Noda, E. Kominami, Y. Ohsumi, T. Yoshimori, LC3, a mammalian homologue of yeast Apg8p, is localized in autophagosome membranes after processing, EMBO J. 19 (2000) 5720–5728.
[74] A. Biederbick, H.F. Kern, H.P. Elsasser, Monodansylcadaverine (MDC) is a specific in vivo marker for autophagic vacuoles, Eur. J. Cell Biol. 66 (1995) 3–14.
[75] D.B. Munafo, M.I. Colombo, A novel assay to study autophagy: regulation of autophagosome vacuole size by amino acid deprivation, J. Cell Sci. 114 (2001) 3619–3629.
[76] D.M. Ward, J. Pevsner, M.A. Scullion, M. Vaughn, J. Kaplan, Syntaxin 7 and VAMP-7 are soluble *N*-ethylmaleimide-sensitive factor attachment protein receptors required for late endosome-lysosome and homotypic lysosome fusion in alveolar macrophages, Mol. Biol. Cell 11 (2000) 2327–2333.
[77] V. Rossi, D.K. Banfield, M. Vacca, L.E. Dietrich, C. Ungermann, M. D'Esposito, T. Galli, F. Filippini, Longins and their longin domains: regulated SNAREs and multifunctional SNARE regulators, Trends Biochem. Sci. 29 (2004) 682–688.
[78] S. Coco, G. Raposo, S. Martinez, J.J. Fontaine, S. Takamori, A. Zahraoui, R. Jahn, M. Matteoli, D. Louvard, T. Galli, Subcellular localization of tetanus neurotoxin-insensitive vesicle-associated membrane protein (VAMP)/VAMP7 in neuronal cells: evidence for a novel membrane compartment, J. Neurosci. 19 (1999) 9803–9812.
[79] P. Alberts, R. Rudge, I. Hinners, A. Muzerelle, S. Martinez-Arca, T. Irinopoulou, V. Marthiens, S. Tooze, F. Rathjen, P. Gaspar, T. Galli, Cross talk between tetanus neurotoxin-insensitive vesicle-associated membrane protein-mediated transport and L1-mediated adhesion, Mol. Biol. Cell 14 (2003) 4207–4220.
[80] S. Martinez-Arca, S. Arold, R. Rudge, F. Laroche, T. Galli, A mutant impaired in SNARE complex dissociation identifies the plasma membrane as first target of synaptobrevin 2, Traffic 5 (2004) 371–382.
[81] C. Thery, M. Boussac, P. Veron, P. Ricciardi-Castagnoli, G. Raposo, J. Garin, S. Amigorena, Proteomic analysis of dendritic cell-derived exosomes: a secreted subcellular compartment distinct from apoptotic vesicles, J. Immunol. 166 (2001) 7309–7318.
[82] T. Galli, T. Chilcote, O. Mundigl, T. Binz, H. Niemann, C.P. De, Tetanus toxin-mediated cleavage of cellubrevin impairs exocytosis of transferrin receptor-containing vesicles in CHO cells, J. Cell Biol. 125 (1994) 1015–1024.
[83] E. Link, H. McMahon, M.G. Fischer von, S. Yamasaki, H. Niemann, T.C. Sudhof, R. Jahn, Cleavage of cellubrevin by tetanus toxin does not affect fusion of early endosomes, J. Biol. Chem. 268 (1993) 18423–18426.
[84] C. Harding, J. Heuser, P. Stahl, Receptor-mediated endocytosis of transferrin and recycling of the transferrin receptor in rat reticulocytes, J. Cell Biol. 97 (1983) 329–339.
[85] J. Zhang, M.S. Randall, M.R. Loyd, F.C. Dorsey, M. Kundu, J.L. Cleveland, P.A. Ney, Mitochondrial clearance is regulated by Atg7-dependent and -independent mechanisms during reticulocyte maturation, Blood 114 (2009) 157–164.
[86] M. Kundu, T. Lindsten, C.Y. Yang, J. Wu, F. Zhao, J. Zhang, M.A. Selak, P.A. Ney, C.B. Thompson, Ulk1 plays a critical role in the autophagic clearance of mitochondria and ribosomes during reticulocyte maturation, Blood 112 (2008) 1493–1502.